# Lung epithelial tip progenitors integrate Glucocorticoid and STAT3-mediated signals to control progeny fate

Usua Laresgoiti[1], Marko Z. Nikolić[1], Chandrika Rao[2], Jane L. Brady[1], Rachel V. Richardson[3], Emma J. Batchen[3], Karen E. Chapman[3] and Emma L. Rawlins[1]

[1] Wellcome Trust/CRUK Gurdon Institute, Wellcome Trust/MRC Stem Cell Institute, Department of Pathology, University of Cambridge, Cambridge, CB2 1QN, UK.

[2] Present address: MRC Centre for Regenerative Medicine, Institute for Stem Cell Research, School of Biological Sciences, University of Edinburgh, 5 Little France Drive, Edinburgh EH16 4UU, UK.

[3] Centre for Cardiovascular Science, Queen's Medical Research Institute, University of Edinburgh, Edinburgh, EH16 4TJ, UK.

**Contact:** e.rawlins@gurdon.cam.ac.uk

**Key words:** glucocorticoid, Stat3, mouse, human, lung development

**Summary Statement:** During lung alveolar development Glucocorticoid Receptor and STAT3 signalling act in parallel, but cross-regulated, pathways to promote epithelial differentiation.

**SUMMARY**

Insufficient alveolar gas exchange capacity is a major contributor to lung disease. During lung development, a population of distal epithelial progenitors first produce bronchiolar-fated and subsequently alveolar-fated progeny. The mechanisms controlling this bronchiolar to alveolar developmental transition remain largely unknown. We developed a novel grafting assay to test if lung epithelial progenitors are intrinsically programmed or if alveolar cell identity is determined by environmental factors. These experiments revealed that embryonic lung epithelial identity is extrinsically determined. We show that both glucocorticoid and STAT3 signalling can control the timing of alveolar initiation, but that neither pathway is absolutely required for alveolar fate specification; rather, glucocorticoid receptor and STAT3 work in parallel to promote alveolar differentiation. Thus, developmental acquisition of lung alveolar fate is a robust process controlled by at least two independent extrinsic signalling inputs. Further elucidation of these pathways may provide therapeutic opportunities for restoring alveolar capacity.

**INTRODUCTION**

The gas exchange capacity of the lung is determined by its functional alveolar surface area. During mouse lung development the early phase (pseudoglandular ~E12.5–15.5) of branching morphogenesis has been mapped in great detail and produces the bronchiolar (conducting airway) tree (Short et al., 2013). During later morphogenesis (canalicular stage ~E16.5-17.5), although the pattern is less well-defined, branching continues to produce the framework for future alveolar development (Alanis et al., 2014). The final size of the gas exchange surface is therefore likely to be strongly influenced by the extent of morphogenesis in the canalicular phase of lung development. Defining the mechanisms which control the developmental transition between bronchiolar and alveolar morphogenesis may ultimately permit manipulation of the size of the alveolar surface for therapeutic purposes.

Definitive lineage-tracing experiments have shown that during lung development the distal tip epithelial cells comprise a multipotent progenitor population (Alanis et al., 2014; Desai et al., 2014; Rawlins et al., 2009a). Tip progenitors are defined by a specific molecular signature, including high levels of SOX9 and ID2. During the pseudoglandular stage their descendants exit the distal tip as $SOX2^{+}$ bronchiolar progenitors and from ~E16.5, during the canalicular stage, their descendants leave the distal progenitor pool as $SOX2^{-}$ alveolar progenitors. Distal progenitors persist at the edge of the lungs until late E17.5/early E18.5, after which tip structures can no longer be detected. Recent molecular experiments have shown that from ~E16.5 distal

progenitors express low levels of markers of both type I and II alveolar epithelial cells (AT1 and AT2) (Desai et al., 2014; Treutlein et al., 2014). Maturation of AT1 and 2 cells likely occurs as $SOX2^-$ alveolar progenitors down-regulate markers of one lineage whilst up-regulating those of the other.

It has been known for many years that glucocorticoid signalling can promote maturation of alveolar cells into functional AT1 and 2 cells. *Glucocorticoid Receptor* (*Nr3c1*, here *GR*) null lungs produce fewer AT1 and 2 cells and synthetic glucocorticoids are routinely used to promote alveolar maturation in infants at risk of premature birth (Cole et al., 2004). A recent study showed that precocious administration of glucocorticoid during mouse lung development promotes the transition from bronchiolar to alveolar fate in the distal progenitors. Moreover, alveolar initiation was delayed in $GR^{-/-}$ mutant lungs, resulting in an extra round of bronchiolar branching (Alanis et al., 2014). Hence GR-mediated signalling controls the timing of alveolar initiation. However, GR signalling is not absolutely necessary for distal progenitor alveolar fate, or alveolar differentiation, and additional mechanisms must also regulate these processes.

To establish whether an intrinsic mechanism or external factors trigger the bronchiolar to alveolar developmental transition during normal development, we developed a heterochronic grafting assay. These experiments showed that non-cell autonomous signalling plays a major role in determining progeny fate of $SOX9^+$ distal tip cells. We investigated the underlying molecular mechanisms and present evidence that STAT3 and GR act in parallel during lung alveolar initiation and are individually sufficient to promote alveolar differentiation.

## RESULTS

### Expression of alveolar-fate markers during mouse lung embryonic development

It was recently reported that alveolar gene expression begins in distal tip epithelial progenitors before overt morphological signs of alveolar differentiation (Desai et al., 2014; Jain et al., 2015; Treutlein et al., 2014). We performed an expression time-course of AT1 and 2 cell markers from E15.5 to E18.5 in wild-type lungs, providing a reference for assessing the extent of alveolar specification/differentiation under experimental conditions. SOX2 and SOX9 are well-established markers of the differentiating bronchioles and tip progenitors (Fig. 1A). We observed very low, variable, levels of LPCAT1 (Lysophosphatidylcholine acyltransferase 1) in E15.5 lung sections (Fig. 1A). It is then robustly detected in tip progenitors from E16.5 and upregulated further in

differentiating AT2 cells, consistent with previous reports (Chen et al., 2006; Nakanishi et al., 2006). This makes LPCAT1 expression a useful marker of alveolar fate in distal tip progenitors.

Pro-SFTPC (Surfactant protein C, pro-SPC) is expressed throughout the lung epithelium from the pseudoglandular stage (Wuenschell et al., 1996). We observed that it is also upregulated in the distal epithelial progenitors at E16.5 and subsequently in differentiating AT2 cells (Fig. 1B). The AT2 cell-specific transcription factor CEBPA (C/EBPα) is first detected in the nucleus of a sub-set of distal epithelial progenitors from E16.5 and then upregulated in differentiating AT2 cells (Fig. 1B) as previously reported (Martis et al., 2006). Earlier, weaker, expression at E15.5 is not nuclear, making nuclear CEBPA a marker of alveolar fate in the distal progenitors. We also observed nuclear CEBPA staining in the bronchioles from E17.5 (Fig. 1B). A recent report has suggested that CEBPA functions redundantly with CEBPB to promote airway differentiation (Roos et al., 2012). We hypothesize that the airway CEBPA staining we observe reflects a second site of expression and therefore do not use this protein as a specific marker of developing alveolar fate.

Similar to pro-SFTPC, the type 1 cell marker PDPN (Podoplanin, T1α) is weakly expressed in the distal progenitors from E15.5 and upregulated in differentiating AT1 cells (Fig. 1C,D). By contrast, LAMP3 (Lysosomal associated membrane protein 3) is expressed strongly in differentiated AT2 cells, but could not be detected robustly in distal progenitors. Rather, at E16.5 LAMP3 is expressed at low levels in cells adjacent to the distal progenitor domain, with levels increasing in these cells at E17.5 (Fig. 1C,D). This makes LAMP3 useful as a marker of early AT2 differentiation, rather than alveolar fate within the distal progenitor population.

The AT1-specific transcription factor, HOPX (Hop homeobox) could not be detected in the distal progenitors. However, it is robustly detected from E16.5 in cells that had exited the distal progenitor domain, but never in the $SOX2^{+}$ differentiating bronchiolar cells (Fig. 1E,F). We noted that cells which have exited the distal progenitor domain by E17.5 reproducibly express either LPCAT1 or HOPX, but not both, suggesting that they are already starting to differentiate along AT1 or AT2 lineages (Fig. 1G). By contrast, cells adjacent to the distal tip at both E16.5 and E17.5 co-express LPCAT1 and HOPX. Relative quantitation of the expression of LPCAT1, LAMP3, HOPX and PDPN (Fig. S1) is in agreement with our descriptions based on visual inspection of the images.

Therefore, and consistent with recent reports, we have found that distal tip progenitors begin to express some markers of alveolar fate at approximately E16.5 (CEBPA, LPCAT1, PDPN protein). By contrast, other protein markers (LAMP3, HOPX) cannot be robustly detected until cells have exited the distal progenitor domain. This timing of alveolar marker expression agrees with the available lineage-tracing data which shows that the distal progenitor cells only produce alveolar-fated (and not bronchiolar-fated) descendants from ~E16.5 onwards (Alanis et al., 2014; Desai et al., 2014; Rawlins et al., 2009a). We hypothesized that the distal progenitors respond to an extrinsic signalling cue to initiate the alveolar programme of development. Alternatively, the progenitors could be intrinsically, cell autonomously, programmed to produce alveolar progeny from approximately E16.5, similar to the temporal production of specific cell identities from neural stem/progenitors in the developing vertebrate nervous system (Livesey and Cepko, 2001).

**Heterochronically-grafted lung epithelial distal progenitors can respond to signals from their local environment and alter descendant cell fate**

To distinguish between our alternative hypotheses for extrinsic versus intrinsic control of distal progenitor fate we asked two related questions. Firstly, is the alveolar fate of the E16.5 $SOX9^+$ distal progenitors fixed, or can they respond to local environmental cues likely from the mesenchyme and reactivate a bronchiolar pathway? Secondly, can bronchiolar-fated already differentiating $SOX2^+$ stalk cells respond to environmental cues from the mesenchyme and produce alveolar-fated descendants? We microdissected pure populations of tip and stalk cells (Fig. S2). Then established a grafting assay to place E12.5 or E16.5 tip, or stalk, ubiquitous-$Tomato^+$ epithelium into the mesenchyme of unlabelled E12.5 host lungs. Hosts were cultured on a membrane to test the response of the grafted cells to their new environment (Fig. 2A). The grafts integrated into the host lungs, were surrounded by host mesenchyme, increased in size over time, and frequently formed a lumen (Fig. 2A',A'' 220/232 [95%] differentiated grafts had a lumen). Although the stalk samples we dissected always contained some adjacent mesenchyme (Fig. S2), we were unable to detect grafted mesenchymal cells at the end of the culture period suggesting that they did not survive. Grafts were identified based on Tomato expression and scored as bronchiolar, mixed (broncho-alveolar), or alveolar-fated by immunostaining alternate slides of serially-sectioned host lung/graft for SOX2/acetylated-tubulin (ACT) (bronchiolar markers), or LPCAT1/PDPN (alveolar markers). Grafts were scored as mixed if they contained distinct bronchiolar and alveolar regions each greater than 10 cells in size (Fig. 2B-G). Overall differentiation efficiency was 98% (232/237 recovered grafts had differentiated).

As a positive (isochronic) control we grafted E12.5 tips into E12.5 hosts. Addition of a synthetic glucocorticoid, such as Dexamethasone (Dx), is necessary to produce differentiated alveolar cells from E12.5 lungs grown in culture. However, Dx has also been shown to promote tip progenitor alveolar fate (Alanis et al., 2014). We therefore cultured host lungs without Dx, or in the presence of Dx from culture day 4 or 5, to allow production of more mature alveolar cells but to minimise precocious alveolar fate specification (Fig. 2A). Previous lineage-labelling experiments showed that ~80% of individual distal tip cells labelled in vivo at E12.5 generate mixed clones of both bronchiolar and alveolar descendants (Rawlins et al., 2009a). In our isochronic control experiments (E12.5 tip grafted into E12.5 host), we obtained approximately 20% bronchiolar, 40% mixed and 40% alveolar-fated grafts (Fig. 2B-D,H), consistent with the position of the graft influencing cell fate. By contrast, E12.5 stalks grafted into E12.5 hosts were more likely to be bronchiolar-fated, although mixed and alveolar-fated grafts were also observed (Figs. 2H,S3: $p=0.0075$). Moreover, these mixed and alveolar-fated stalk grafts expressed the AT2 specific marker LAMP3 (Fig. S3H-J). This surprising result suggests that although stalks have initiated a bronchiolar developmental programme, they retain some plasticity to respond to extrinsic cues from the local environment and alter fate. Overall the results obtained with the two growth conditions (no Dx, or Dx from culture day 4/5) were very similar (Fig. 2H).

We next performed heterochronic grafting experiments in which E16.5 tip, or stalk, cells were grafted into E12.5 lungs grown without Dx, or with a short period of Dx-exposure (Fig. 2A). Consistent with their developmental age, the E16.5 tip grafts were more likely to produce only alveolar-fated descendants than their E12.5 counter-parts (Fig. 2E,F,G,I: $p=0.0438$). Nevertheless, bronchiolar-fated and mixed broncho-alveolar fated grafts were also observed showing that the E16.5 tip progenitors, which normally only produce alveolar descendants, can respond to local environmental cues and change their behaviour appropriately. The E16.5 stalk grafts behave very similarly to the E12.5 stalk grafts in this assay, although with somewhat less plasticity in that they never produce only alveolar-fated descendants (Figs. 2I, S3).

We conclude that both distal progenitor cells and differentiating stalk cells can respond to their local environment and produce appropriate descendants. This supports the hypothesis that extrinsic signalling, likely from the local mesenchyme is a major determinant of lung epithelial progenitor cell fate. However, older distal tip and stalk cells become more refractory to external cues with time, presumably corresponding to increased levels of differentiation, suggesting that

they have also undergone intrinsic, possibly epigenetic, changes which cell autonomously reduce their capacity to respond to an external signal.

**Glucocorticoid signalling is sufficient, but not necessary, for tip alveolar fate**

What are the extrinsic signals which promote alveolar fate in the tip progenitors? A recent report showed that GR signalling, likely induced by circulating glucocorticoids, was sufficient to promote precocious lung alveolar fate both in vitro and in vivo (Alanis et al., 2014). We therefore tested if GR signalling is also sufficient to promote alveolar fate in our grafting experiments. Host lungs were exposed to Dx throughout the culture period and the fate of the grafts determined (Fig. 3A-C). In these conditions almost 100% of distal tip grafts produced alveolar-fated descendants. Moreover, attenuated $PDPN^{+}$ cells with the appearance of AT1 cells differentiated in these grafts (Fig. 3B), consistent with sustained glucocorticoid signalling being necessary for AT1 differentiation. By contrast, grafted stalk cells were less likely to respond to the signal by producing alveolar descendants (Fig. 3C: p=0.0016). However, in the presence of Dx, grafted stalks were more likely to produce alveolar-fated or mixed broncho-alveolar-fated descendants than grafted stalks without Dx, or when Dx was added late in the culture period (compare Fig. 3C with 2H,I: p=0.0067). These experiments confirm the ability of GR signalling to promote alveolar fate. In addition, they show that the undifferentiated distal tip cells are completely plastic in their ability to respond to this signal.

Is GR signalling necessary for tip progenitors to initiate alveolar gene expression? We observed that wild-type E12.5 lungs grown in vitro with Dx initiated wide-spread LPCAT1 expression by culture day 3. By contrast, in the absence of Dx, LPCAT1 was only robustly detected at culture day 5 (Fig. 3D). Thus, addition of Dx promotes/accelerates alveolar gene expression, but is not an absolute requirement for alveolar fate initiation to occur in vitro. However, it is possible that embryonic lungs can also endogenously synthesise glucocorticoids de novo (Boucher et al., 2014). We therefore examined the timing of expression of alveolar fate markers in developing lungs from $GR^{-/-}$ embryos (Fig. 3E). We observed that, as previously published, the $GR^{-/-}$ lungs were developmentally delayed. Nevertheless, they did express markers of both tip alveolar fate (LPCAT1, PDPN) and alveolar differentiation (HOPX, LAMP3), albeit delayed, relative to wild-type. This shows that GR signalling affects the timing of alveolar fate acquisition, but is not essential for either tip progenitor alveolar fate induction, or initial alveolar differentiation. We therefore hypothesized that other extrinsic signals acting prior to, or in parallel with,

glucocorticoids also promote alveolar fate. Moreover, based on our in vitro grafting results we hypothesized that these signals would be expressed within the lung itself.

**Overexpression of *Stat* genes promotes alveolar fate/differentiation in cultured lungs**

To search for candidate signalling pathways that control alveolar fate, we isolated E11.5 and E17.5 distal tip cells, with a small number of their immediate progeny, and compared their transcriptomes using gene expression microarrays (Fig. 4A). We performed Gene Ontology (GO) analysis of the genes enriched in E17.5 samples and found that the most prominent GO classes were: Immune System Process; Immune Response; Response to External Stimulus; Response to wounding. Within these classes it was particularly noticeable that components of cytokine signalling were enriched in the older samples (Fig. 4B). Cytokine signalling is reportedly important for lung maturation (Ikegami et al., 2008; Matsuzaki et al., 2008; Moreno-Barriuso et al., 2006). We therefore tested various cell autonomous transcription factors (TFs) for their ability to promote alveolar fate in vitro with a focus on STAT proteins, which are important mediators of cytokine signalling. Adenoviruses carrying GFP, or a TF + GFP, were microinjected into the lumen of wild-type E12.5 lungs. This resulted in labelling of both tip and stalk cells within 72 hours. Lungs were then cultured for 8 days in the presence of Dx, fixed and sectioned, and the location of $GFP^+$ cells scored as alveolar or bronchiolar (Fig. 4C).

$GFP^+$ cells transduced by control adenovirus were equally likely to be located in the alveoli or bronchioles (normalised $GFP^+$ alveolar : bronchiolar ratio of 1; Fig. 4D, E). This was unchanged by $NOTCH1^{ICD}$ (Notch1 intracellular domain), consistent with previous in vivo results (Guseh et al., 2009). Similarly, CEBPA, which is expressed in E16.5 distal progenitors and also in bronchiolar cells from E17.5 (Fig. 1B), was unable to affect the location of $GFP^+$ cells. By contrast, we found that over-expression of STAT3, 5A, or 6, or CITED2, a TF required for AT2 differentiation (Xu et al., 2008a), was each sufficient to increase the $GFP^+$ alveolar : bronchiolar ratio to ~2 (Fig. 4E). Dividing $GFP^+$ cells were detected only rarely in our cultures (Fig. 4F) and we could find no evidence for effects of the transcription factors on proliferation rate. We confirmed that the transduced cells were differentiating to AT1 and 2 fate in our culture conditions (Fig. 4G,H). As an approximation to the relative production of AT2 versus AT1 cells in these experiments we scored the number of alveolar $GFP^+$ cells which co-expressed high levels of pro-SFTPC (Fig. 4I,J). There was no evidence for a change in the percentage of $(GFP,pro\text{-}SFTPC)^+$ co-expressing cells when CITED2 or STATs were overexpressed. However, as a

positive control for this assay, NOTCH1$^{ICD}$ reduced AT2 cell differentiation consistent with published data (Guseh et al., 2009).

The effects of STAT proteins on alveolar location of GFP$^+$ cells in these experiments could either be mediated through an undetected change in the differential proliferation rate between transduced bronchiolar versus alveolar progenitors, or through promotion of alveolar fate. Analysis of STAT6 protein location in wild-type embryonic lungs showed it was predominantly bronchiolar. We therefore made lung epithelial-specific deletions of *Stat3* and *Stat5* to test if they were required for alveolar development.

**Lung epithelial specific knock-out of *Stat3* results in a short delay in alveolar development.**
A detailed time-course of phosphorylated-STAT3 (active, pSTAT3) expression showed it was undetectable at E15.5, but appeared weakly in the tip progenitors from E16.5 (arrowheads in Fig. 5B,C) and more strongly in differentiating alveolar cells which had exited the distal progenitor pool (Fig. 5A-D, S4). pSTAT3 was also observed in the bronchioles, consistent with a role in airway differentiation (Tadokoro et al., 2014). The majority of pSTAT3$^+$ cells were E-CAD$^+$.

We generated *Nkx2.1-Cre; Stat3$^{\Delta/fx}$* (cKO) and control *Nkx2.1-Cre; Stat3$^{+/fx}$*, or *Stat3$^{+/fx}$*, embryos to remove STAT3 specifically from the developing lung epithelium. qRT-PCR showed that *Stat3* mRNA levels were decreased in the cKO lungs compared to controls, but recombination was not completely efficient (Fig. 5E). pSTAT3 immunostaining in E17.5 cKO and control lungs showed that recombination in the cKO lungs was highly variable, with some having an almost complete loss of pSTAT3 and others being largely unaffected (Fig. 5F-H). Examination of reporter gene expression in *Nkx2.1-Cre; Rosa26R-fGFP* lungs gave a similar, highly variable, result (Fig. S4A).

To assess a wide range of alveolar fate and differentiation markers we performed qRT-PCR from *Stat3*cKO and control lungs at E16.5 and E18.5. At E16.5, lungs from cKO mice exhibited >2-fold decreases in the level of *SftpD* and *Aqp5*, previously reported as markers of mature AT1 and AT2 cells (Desai et al., 2014) (Fig. 5I,J). However, *SftpD* and *Aqp5* levels were normal at E18.5 and other markers did not change significantly (Fig. 5I-K, S4C). These results are suggestive of a short delay in alveolar differentiation. To confirm this, we performed a detailed antibody staining time-course in *Stat3* cKO and control lungs, co-staining with pSTAT3 to assess the extent of recombination. We observed a modest increase in the number of SOX9$^+$ distal tips in the cKO lungs at E17.5 (Fig. 5L,M; 0.1 ± 0.01, versus 0.18 ± 0.03 tips per 200 μm$^2$, n=3 lungs), but tip

number appeared normal by E18.5. Expression of the key alveolar fate and differentiation markers commenced at the expected times, with up-regulation in differentiating cells by E18.5 (Fig. 5N-W, S4D-H). These subtle phenotypes are consistent with a brief developmental delay in the *Stat3* cKO lungs.

STAT5A is expressed strongly in a sub-set of distal tip progenitor cells at E16.5 (Fig. S5A). We generated *Nkx2.1-Cre; Stat5*$^{\Delta/fx}$ (cKO) and control *Nkx2.1-Cre; Stat5*$^{+/fx}$, or *Stat5*$^{+/fx}$, embryos to remove STAT5A and B from the developing lung epithelium. Similar to *Stat3*, qRT-PCR confirmed the partial deletion of *Stat5* (Fig. S5B). However, we were unable to detect any phenotype in the *Stat5* cKO lungs (Fig. S5B-F). This indicates that STAT5 is not required for alveolar fate specification or differentiation. These experiments also provide useful controls showing that the subtle phenotypes observed in the *Stat3* cKO lungs were specific to *Stat3* deletion and not a result of non-specific Cre activity.

**Widespread STAT3 activation accelerates lung alveolar differentiation**

We asked if STAT3 activation by ectopic ligand was sufficient to promote alveolar differentiation. We established a culture system in which E15.5 wild-type lung slices were incubated at air-liquid interface in medium containing 5% FBS. In the presence of Dx robust alveolar differentiation was observed after 3 days, with distinct AT1 and 2 cells arranged around saccular structures (Fig. 6A). To test the ability of the Interleukin 6 (IL6) family ligands, IL6 and LIF, to induce alveolar differentiation, individual lung slices were split and incubated with, or without, the cytokine for 3 days (Fig. 6B). These experiments were performed with, and without, Dx. Both IL6 and LIF treatment robustly activated STAT3 throughout the lung slices (Fig. 6C). No detectable phenotypic changes were induced by IL6 and LIF in the presence of Dx. In the absence of Dx, control lung slices showed low levels of LPCAT1 and LAMP3 indicating that alveolar fate specification had occurred. However, there was no evidence of AT2 differentiation or saccule formation. When either IL6 or LIF was added, in the absence of Dx, levels of the more specific AT2 differentiation marker LAMP3 were much higher, compared to controls (Fig. 6D; 9/9 IL6-treated and 6/7 LIF-treated lungs in three independent experiments). HOPX and SOX9 expression were unchanged (Fig. S6). This suggests that AT2 differentiation occurred in response to cytokine signalling, but the overall morphology of the slices remained immature. The effect of IL6 upon AT2 differentiation was consistently more potent than LIF. Oncostatin M (*Osm*) and its receptor (*Osmr*) were also detected in our microarray experiments (Fig. 4B), but addition of

recombinant OSM to the slice cultures did not promote LAMP3 expression (Fig. S6; 0/6 OSM-treated lungs in two independent experiments).

We tested if STAT3 is required to mediate the effects of IL6 in the slice cultures. We cultured *Stat3* cKO and sibling control lungs +/- IL6 and observed that in the absence of STAT3, LAMP3 levels were reduced to those of control lung slices with no IL6 exposure (Fig. 6E). These results suggest that activation of STAT3 signalling by IL6 or LIF is sufficient to promote expression of mature AT2 markers, even in the absence of glucocorticoids.

**GR and STAT3 signalling act in parallel during alveolar development**

We considered the possibility that STAT3 and GR signalling act redundantly in alveolar development and that inactivation of both signalling pathways would result in a stronger phenotype. To test this hypothesis we cultured E12.5 *Stat3* cKO and littermate control lungs for 5 days in the absence of Dx, or in the presence of a glucocorticoid and progesterone antagonist Mifepristone, so that both STAT3 and GR signalling would be decreased (Fig. S7). In both conditions, alveolar fate markers were expressed as expected (Fig. S7) and wholemount analysis indicated that the transition from producing bronchiolar ($SOX2^{+}$) to alveolar-fated ($SOX2^{-}$) descendants occurred at the same time in all genotypes (Fig. S7D). These results suggest that STAT3 and GR signalling are not acting redundantly at these stages of alveolar development.

Our ectopic ligand results (Fig. 6) are consistent with STAT3 acting downstream of GR signalling to mediate some of its effects. We therefore examined pSTAT3 expression in $GR^{-/-}$ and littermate control lungs. At E17.5 the $GR^{-/-}$ lungs had very little pSTAT3 expression consistent with their developmental delay (Fig. 7A). However, by E18.5 the pSTAT3 signal was reproducibly greater in the $GR^{-/-}$ lungs compared to the controls (Fig. 7B). This effect was even more pronounced in an independent litter, which was collected at a slightly later developmental stage (Fig. 7C). The increase in pSTAT3 levels could also be replicated by treating cultured lungs with the glucocorticoid and progesterone antagonist Mifepristone (Fig. S8A). We considered the hypothesis that the increase in pSTAT3 in the *GR* mutants was related to an increase in apoptotic cell death, but were unable to detect a significant increase in the levels of apoptosis measured by cleaved-Caspase 3 staining (Fig. S8B). Interestingly, we observed an increase in LIF protein levels in the $GR^{-/-}$ lungs, possibly partly explaining the increase in pSTAT3 (Fig. S8C).

These data suggest that STAT3 signalling is not directly downstream of GR signalling in a linear pathway. Rather, it is likely that STAT3 and GR signalling act in parallel to promote the differentiation of alveolar cells, but that there is some cross-regulation between the two pathways. Like GR, STAT3 is not absolutely required for alveolar differentiation (Fig. 3). However, ectopic exposure to STAT3 activating ligands was sufficient to promote AT2 differentiation (Fig. 6). Activation of STAT3 signalling could be useful for promoting the maturation of human iPS cell-derived alveolar epithelium, or for human lung regeneration. We therefore examined human embryonic lungs to test whether STAT3 and GR signalling are active at similar stages to mouse lung development (Fig. 7D). We were unable to detect epithelial pSTAT3 in the distal epithelium of pseudoglandular stage human lungs (post conception weeks (pcw) 11 and 14 were tested). However, pSTAT3 was detected strongly in the epithelium of a 17 pcw lung, which had a much more canalicular appearance. We therefore hypothesize that STAT3 signalling plays similar roles in mouse and human lung alveolar development, but further investigation is required to test this idea. By contrast nuclear (active) GR was slightly different between the two species. It was detected strongly in both mesenchyme and epithelium of E16.5 and E18.5 mouse lung as previously reported (Fig. S9A-C), though not at E14.5. However, nuclear GR was already present in the mesenchyme of 8 pcw human embryonic lungs and the distal tip epithelium of 11 and 17 pcw samples (Fig. S9D-F).

## DISCUSSION

Elucidating the cellular and molecular mechanisms that control the induction of alveolar fate in the distal tip progenitors of the embryonic lung, and subsequent alveolar differentiation, will be important for efforts to regenerate the alveolar epithelium. Our grafting experiments have conclusively shown that extrinsic signalling from the surrounding tissue is sufficient to control the fate of the progeny produced by distal lung epithelial progenitors. This is analogous to previous experiments which showed that mesenchymally-derived signals were sufficient to impose a tracheal, or lung, branching pattern on embryonic lung endoderm (Alescio and Cassini, 1962; Shannon, 1994; Shannon et al., 1998). Interestingly, the differentiating stalk cells were surprisingly plastic and could be induced to produce alveolar fated descendants, even in the absence of exogenous Dx. The E12.5 stalks were more plastic than their more differentiated E16.5 counter-parts. The mechanisms underlying this plasticity, particularly the extent of any epigenetic changes, will be an interesting topic of future study.

We present evidence that STAT3 and GR signalling are individually sufficient to promote alveolar differentiation and that they act in parallel during normal embryonic lung development (Fig. 7E). Our results also suggest that lung alveolar initiation is a highly robust process during which the GR and STAT3 pathways are redundant with other, yet to be identified, signalling modules. We observed that STAT3 and STAT5A have similar expression patterns and modest lung phenotypes and one possibility is that they are redundant in alveolar development, although we could find no evidence for compensatory upregulation/activity of either protein (Figs. S4G, S5F). The two genes are located adjacently on chromosome 11 and testing this hypothesis will require the development of additional tools for gene deletion.

We focus on the initial stages of lung alveolar differentiation and show that neither STAT3 nor GR are absolutely required, individually or redundantly together, for this process. Nevertheless, experimental activation of either pathway can promote distal progenitor alveolar fate, or AT2 differentiation, depending on timing. Glucocorticoid levels rise dramatically in the mouse foetus following onset of steroidogenesis at ~E15. We propose that during normal mouse lung development both STAT3 and GR signalling promote alveolar differentiation from ~E16.5 onwards (Fig. 7E). GR has a greater role and is also absolutely required for the later stages of alveolar differentiation (Cole et al., 2004). However, both pathways are redundant with other signalling mechanisms at the early stages of alveolar differentiation. When GR signalling is disrupted we observe that signalling via STAT3 is increased, likely in an attempt to compensate. In support of this idea, ectopic STAT3 activity in vitro can promote AT2 differentiation in the absence of exogenous Dx. Interestingly, GR and STAT proteins have been reported to act together in multiple settings via several molecular mechanisms including joint transcriptional activation/repression (Engblom et al., 2007; Langlais et al., 2012) and control of nuclear localisation (Shin and Reich, 2013).

Finally, we present evidence that STAT3 and GR signalling are active at the canalicular stage of normal human embryonic development, supporting the idea that their functions are conserved across species. It will be important to test if manipulating STAT3 can promote improved AT2 differentiation in human lung iPS-derived cultures, or even directly in the lungs of premature infants. Our data show that alveolar fate determination is a highly robust process, likely involving additional extrinsic signalling inputs as well as STAT3 and GR. It will be important to define these pathways for human and mouse embryonic lungs.

## MATERIALS AND METHODS

### Animals

All experiments were approved by University of Cambridge and University of Edinburgh local ethical review committees and conducted according to Home Office project licenses PPL80/2326, 70/812 and 70/7874. Mouse strains *Rosa26R-mT/mG* (Muzumdar et al., 2007), *Nr3c1*$^{Gt(ESKN92)Hgs}$ (*GR* null) (Michailidou et al., 2008), *Stat3*$^{fx}$ (Alonzi et al., 2001), *Stat5*$^{fx}$ (Cui et al., 2004), *Nkx2.1-Cre* (Xu et al., 2008b), *Id2-CreER* (Rawlins et al., 2009a) and *Rosa26R-fGFP* (Rawlins et al., 2009b) have been described. *Stat3*$^{\Delta/+}$ and *Stat5*$^{\Delta/+}$ were generated by crossing floxed alleles to *Zp3-Cre* (de Vries et al., 2000). Transgenic strains were maintained on a C57Bl/6J background (at least N4 back-crosses, or >20 back-cross generations for *GR*$^{+/-}$). Wild-type mice were out-bred MF1 strain.

### Human Material

The human embryonic and foetal material was provided by the Joint MRC/Wellcome Trust (grant 099175/Z/12/Z) Human Developmental Biology Resource (www.hdbr.org), or collected at Addenbrooke's Hospital (Cambridge, UK) under permission from NHS Research Ethical Committee (96/085). Samples used had no known genetic abnormalities.

### Lung cultures and manipulations

All in vitro cultures were performed in at least 3 independent experiments unless otherwise stated. Mouse E12.5 lungs were cultured on Whatman Nucleopore filters 10 μm pore size (Millipore) in BGJ/b medium (Sigma) at 37°C, 5% $CO_2$ up to 8 days. E15.5 lungs were cut into slices using a razor blade and cultured up to 3 days on filters in BGJ/b medium with 5% FBS (Gibco). Dexamethasone (Dx, Sigma) was used at 50 nM for E12.5 lungs and 100 nM for E15.5 slices. Mifepristone (Sigma) was used at 3 μM. Recombinant IL6 (R and D Systems) and LIF (Millipore) 10 ng/ml; recombinant OSM (R and D systems) 25 ng/ml.

For grafting, tip and stalk cells were microdissected from *Rosa26R-mT/mG* heterozygous embryos using tungsten needles following 5 minutes in Dispase (Gibco, 16 U/ml final concentration) room temperature. Stalk cells were taken from a region of future bronchiole 2-3 branches above the distal tip. Microdissected epithelial tips and stalks were washed in Phytohemagglutin PHA-P (Lectin from *Phaseolus vulgaris*, Sigma, 0.2 mg/ml final concentration) and inserted into a pocket made in the mesenchyme of a wild-type E12.5 lung on a filter. Grafts were always placed in approximately the centre of the host lung.

For adenovirus injections, E12.5 lungs were submerged in PBS and microinjected with $2x10^{10}$ IFU (Infections Units)/ml virus mixed with trypan blue (4:1 ratio). The lumen of the branching tree was filled (~10 nl) by microinjecting with a Nanoject II Auto-Nanoliter Injector. Lungs were incubated at room temperature in PBS at least 1 hour before transfer to filter for culturing.

**Immunostaining**

E15.5-18.5 mouse lungs were fixed 1-2 hours in 4% paraformaldehyde at 4°C. Human lungs were fixed overnight. Samples were washed in PBS, sucrose protected, embedded in OCT (Optimum Cutting Temperature Compound, Tissue Tek) and sectioned at 8 μm. Primary antibodies: acetylated tubulin (mouse, 1:3000, Sigma, T7451), CEBPA (rabbit, 1:500, Santa Cruz, sc-61), cleaved caspase 3 (rabbit, 1:100, AbCam, ab2302), E-cadherin (rat, 1:1000, Invitrogen, 13-1900; or mouse, 1:1000, BD, 610182), GFP (chick, 1:1000, AbCam, AB13970), GR (rabbit, 1:100, Santa Cruz, sc-1004), HOPX (rabbit, 1:50, Santa Cruz, sc-30216, clone FL-73), KI67 (mouse, 1:200, BD, 550609), LAMP3 (rat, 1:100, Dendritics, DDX0192, clone 1006F7.05), LIF (goat, 1:100, R and D Systems, AB-449-NA), LPCAT1 (rabbit, 1:500, Proteintech), PDPN (hamster, 1:1000, DSHB, 8.1.1), RFP (rabbit, 1:250, Rockland, 600-401-379), pro-SFTPC (rabbit, 1:500, Millipore, AB3786), SOX2 (goat, 1:250, Santa Cruz, sc-17320, clone Y-17), SOX9 (goat, 1:200, R and D Systems, AF3075), pSTAT3-Tyr705 (rabbit, 1:200, Cell Signalling, 9145), STAT5a (rabbit, 1:20, AbCam, ab7968). Antigen retrieval was by boiling in 10 mM sodium citrate, pH 6 for mouse anti-E-CAD, rabbit-anti-HOPX, mouse-anti-KI67, goat-anti-SOX2, rabbit-anti-pSTAT3. Alexa-Fluor conjugated secondary antibodies (1:2000, Life Technologies). DNA (Dapi, Sigma). Mounting in Fluoromount (Sigma).

pSTAT3 was amplified using the TSA Plus Cyanine 3 Kit (PerkinElmer NEL744001KT). For double-rabbit primary staining (HOPX/LPCAT1; HOPX/pSTAT3; HOPX/STAT2; LPCAT1/pSTAT3) an excess (40 μg/ml) of Fab fragment donkey anti-rabbit IgG (H+L) (Jackson Immunoresearch, 711-007-003) was used to block the first primary.

For wholemounts, cultured E12.5+5 days mouse lungs were fixed 2 hours in 4% paraformaldehyde at 4°C, washed in PBS with 2% non-fat milk powder and 0.2% triton and stained with E-cadherin (rat, 1:1000, Invitrogen, 13-1900), SOX2 (goat, 1:250, Santa Cruz, sc-17320, clone Y-17), SOX9 (rabbit, 1:1000, Millipore, AB5532). Samples were passed through a glycerol series before mounting in Vectashield (Vector Labs).

**Microscopy and image scoring**

Slides were imaged on a Zeiss AxioImager compound microscope, or Olympus FV1000 confocal microscope where stated. Cell numbers were scored manually in Fiji (ImageJ). Protein expression levels in Figure 1 were quantified using a custom macro for ImageJ (Schneider et al., 2012) (Gurdon Institute website) to measure the area of signal in each channel and calculate the proportion of the cell area containing signal for each. The DAPI channel was Gaussian blurred and Huang thresholded to give a representation of the cell area from the nuclear signal, other channels were maximum entropy thresholded (Kapur et al., 1985) to give the area containing signal above background. This gave a reliable metric for assessing the relative number of cells positive for each marker which matches our visual assessment.

For grafting experiments, serial sections were cut through the entire lung and even numbered slides stained to show bronchiolar fate and odd-numbered for alveolar fate. Grafts were tracked in each section and scored as bronchiolar, alveolar, or mixed. Grafts were scored as mixed if they contained two clearly separated bronchiolar and alveolar regions each greater than 10 cells. Statistical tests were two-tailed Fisher's exact tests.

For adenovirus experiments, epithelial cells were scored based on their location and E-CAD staining as bronchiolar (columnar, lower intensity) or alveolar (squamous, higher intensity) and for the presence or absence of nuclear GFP. The normalised $GFP^+$ alveolar : bronchiolar ratio was calculated by [($GFP^+$ alveolar epithelial cells/ all alveolar epithelial cells scored) / ($GFP^+$ bronchiolar epithelial cells / all bronchiolar epithelial cells scored)]. $GFP^+$ alveolar cells were later scored for the presence, or absence of pro-SFTPC in images taken with a defined exposure time. Images were scored by two independent investigators who were blind to the experimental group. Statistical tests were two-tailed t-tests with unequal variance.

**RT-qPCR and microarrays**

Total RNA was extracted using Qiagen RNEasy Mini Kit and cDNA was synthesised using Superscript III reverse transcriptase (Life Technologies). Primer sequences: *Aqp5* 5'-AGGTGTGTTCAGTTGCCTTCTTC -3' and 5'- AGATGAGGGTGGCCAGGAA-3'; *Cebpa* 5'-GAGCTGAGTGAGGCTCTCATTCT-3' and 5'-TGGGAGGCAGACGAAAAAAC-3'; *Hopx* 5'-TGCCTTCGGAATGCAGATCT -3' and 5'- AGCTCAAGGGCCTGGCTC-3'; *Id2* 5'-AAGGTGACCAAGATGGAAATCCT-3' and 5'-CGATCTGCAGGTCCAAGATGT-3'; *Lamp3*

5’-AATGTGAACGAGTGTTTGTCTGACTA-3’ and 5’-GACGACCACGATGATTGCAA-3’; *Lpcat1* 5’-TTATGGAGGAAGGTCGTGGACTT-3’ and 5’-GAAGCCGCCAGCAAACC-3’; *SftpD* 5’-AGCAGAAATGAAGAGCCTCTCG-3’ and 5’-AGGGTGCAGGTGTTGGGTAC-3’; *Sox9* 5’-GCAGCACTGGGAACAACCA-3’ and 5’-GCTCTGTCACCATAGCTTTTCTCTT-3’; *Stat3* 5’-CAGAGGGTCTCGGAAATTTAACAT-3’ and 5’-CTCCCTAAGGGTCAGGTGCTT-3’; *Stat5a* 5’-TGGCTTTGCACGTTTCACA-3’ and 5’-CACCGCTTTAGCCACAAACC-3’.

For microarray analysis E11.5 tip cells were manually microdissected. $GFP^+$ E17.5 tip cells, with a small number of their immediate progeny, were collected by flow cytometry from *Id2-CreER; Rosa26R-fGFP* embryos exposed to 150 µg/gram mother’s body weight at E16.5. RNA was isolated using the Qiagen RNEasy Mini Kit, amplified and labelled using the Ovation RNA Amplification Kit V2 and FL-Ovation Biotin V2 (NuGEN). Hybridisation to Affymetrix mouse 430.2 microarray chips (5 chips per condition). Data were analysed using the Bioconductor Package in R. Gene Ontology analysis using GOToolbox (http://genome.crg.es/GOToolBox/). Raw data deposited in GEO: GSE75860.

**Adenovirus production**

Adenovirus construction was as previously described (Zhou et al., 2008). Genes were cloned from E16.5 lung cDNA into a shuttle vector containing an internal ribosome entry site linked to nuclear GFP (*IRES-nGFP*), and then into the pAd/CMV/V5-DEST adenoviral vector (Invitrogen). High titer non-replicating virus ($>1 \times 10^{10}$ IFU/ml) was obtained by purification with the Fast-Trap Adenovirus Purification and Concentration Kit (Millipore, FTAV00003). Titer was determined using AdEasy Viral Titer Kit (Agilent Technologies, 972500). Two isoforms of *Stat3* and *Stat5a* were cloned from E16.5 wild-type lungs, both were used (*Stat3.1/Stat3.2*; *Stat5a.1/Stat5a.2*) with indistinguishable results.

## ACKNOWLEDGEMENTS

Richard Butler, Gurdon Institute, for ImageJ programming.

## COMPETING INTERESTS

No competing interests declared.

## AUTHOR CONTRIBUTIONS

UL and MN designed and performed experiments, analysed data and edited the manuscript. CR and JLB performed experiments. RVR, EJB and KEC provided mice and lung samples and assisted with experimental design. ELR conceived and led the project, analysed data, performed experiments and wrote and edited the manuscript.

## FUNDING

Medical Research Council (G0900424, ER), the March of Dimes (5-FY11-119, ER), the Wellcome Trust (093029, ER), Newton Trust (14.07h, ER), Wellcome Trust PhD programme for Clinicians (MN), Postdoctoral Fellowship from the Government of the Basque Country (UL), MRC studentship (RVR), British Heart Foundation Studentship (EJB), COST BM1201. Core grants from the Wellcome Trust (092096) and Cancer Research UK (C6946/A14492).

## REFERENCES


Alanis, D.M., Chang, D.R., Akiyama, H., Krasnow, M.A., Chen, J., 2014. Two nested developmental waves demarcate a compartment boundary in the mouse lung. Nat Commun 5, 3923.

Alescio, T., Cassini, A., 1962. Induction in vitro of tracheal buds by pulmonary mesenchyme grafted on tracheal epithelium. The Journal of experimental zoology 150, 83-94.

Alonzi, T., Maritano, D., Gorgoni, B., Rizzuto, G., Libert, C., Poli, V., 2001. Essential role of STAT3 in the control of the acute-phase response as revealed by inducible gene inactivation [correction of activation] in the liver. Mol Cell Biol 21, 1621-1632.

Boucher, E., Provost, P.R., Tremblay, Y., 2014. Ontogeny of adrenal-like glucocorticoid synthesis pathway and of 20alpha-hydroxysteroid dehydrogenase in the mouse lung. BMC research notes 7, 119.

Chen, X., Hyatt, B.A., Mucenski, M.L., Mason, R.J., Shannon, J.M., 2006. Identification and characterization of a lysophosphatidylcholine acyltransferase in alveolar type II cells. Proc Natl Acad Sci U S A 103, 11724-11729.

Cole, T.J., Solomon, N.M., Van Driel, R., Monk, J.A., Bird, D., Richardson, S.J., Dilley, R.J., Hooper, S.B., 2004. Altered epithelial cell proportions in the fetal lung of glucocorticoid receptor null mice. Am J Respir Cell Mol Biol 30, 613-619.

Cui, Y., Riedlinger, G., Miyoshi, K., Tang, W., Li, C., Deng, C.X., Robinson, G.W., Hennighausen, L., 2004. Inactivation of Stat5 in mouse mammary epithelium during pregnancy reveals distinct functions in cell proliferation, survival, and differentiation. Mol Cell Biol 24, 8037-8047.

de Vries, W.N., Binns, L.T., Fancher, K.S., Dean, J., Moore, R., Kemler, R., Knowles, B.B., 2000. Expression of Cre recombinase in mouse oocytes: a means to study maternal effect genes. Genesis 26, 110-112.

Desai, T.J., Brownfield, D.G., Krasnow, M.A., 2014. Alveolar progenitor and stem cells in lung development, renewal and cancer. Nature 507, 190-194.

Engblom, D., Kornfeld, J.W., Schwake, L., Tronche, F., Reimann, A., Beug, H., Hennighausen, L., Moriggl, R., Schutz, G., 2007. Direct glucocorticoid receptor-Stat5 interaction in hepatocytes controls body size and maturation-related gene expression. Genes Dev 21, 1157-1162.

Guseh, J.S., Bores, S.A., Stanger, B.Z., Zhou, Q., Anderson, W.J., Melton, D.A., Rajagopal, J., 2009. Notch signaling promotes airway mucous metaplasia and inhibits alveolar development. Development 136, 1751-1759.

Ikegami, M., Falcone, A., Whitsett, J.A., 2008. STAT-3 regulates surfactant phospholipid homeostasis in normal lung and during endotoxin-mediated lung injury. J Appl Physiol 104, 1753-1760.

Jain, R., Barkauskas, C.E., Takeda, N., Bowie, E.J., Aghajanian, H., Wang, Q., Padmanabhan, A., Manderfield, L.J., Gupta, M., Li, D., Li, L., Trivedi, C.M., Hogan, B.L., Epstein, J.A., 2015. Plasticity of Hopx(+) type I alveolar cells to regenerate type II cells in the lung. Nat Commun 6, 6727.

Kapur, J.N., Sahoo, P.K., Wong, A.K.C., 1985. A New Method for Gray-Level Picture Thresholding Using the Entropy of the Histogram. Comput Vision Graph 29, 273-285.

Langlais, D., Couture, C., Balsalobre, A., Drouin, J., 2012. The Stat3/GR interaction code: predictive value of direct/indirect DNA recruitment for transcription outcome. Mol Cell 47, 38-49.

Livesey, F.J., Cepko, C.L., 2001. Vertebrate neural cell-fate determination: lessons from the retina. Nat Rev Neurosci 2, 109-118.

Martis, P.C., Whitsett, J.A., Xu, Y., Perl, A.K., Wan, H., Ikegami, M., 2006. C/EBPalpha is required for lung maturation at birth. Development 133, 1155-1164.

Matsuzaki, Y., Besnard, V., Clark, J.C., Xu, Y., Wert, S.E., Ikegami, M., Whitsett, J.A., 2008. STAT3 regulates ABCA3 expression and influences lamellar body formation in alveolar type II cells. Am J Respir Cell Mol Biol 38, 551-558.

Michailidou, Z., Carter, R.N., Marshall, E., Sutherland, H.G., Brownstein, D.G., Owen, E., Cockett, K., Kelly, V., Ramage, L., Al-Dujaili, E.A., Ross, M., Maraki, I., Newton, K., Holmes, M.C., Seckl, J.R., Morton, N.M., Kenyon, C.J., Chapman, K.E., 2008. Glucocorticoid receptor haploinsufficiency causes hypertension and attenuates hypothalamic-pituitary-adrenal axis and blood pressure adaptions to high-fat diet. FASEB J 22, 3896-3907.

Moreno-Barriuso, N., Lopez-Malpartida, A.V., de Pablo, F., Pichel, J.G., 2006. Alterations in alveolar epithelium differentiation and vasculogenesis in lungs of LIF/IGF-I double deficient embryos. Dev Dyn 235, 2040-2050.

Muzumdar, M.D., Tasic, B., Miyamichi, K., Li, L., Luo, L., 2007. A global double-fluorescent Cre reporter mouse. Genesis 45, 593-605.

Nakanishi, H., Shindou, H., Hishikawa, D., Harayama, T., Ogasawara, R., Suwabe, A., Taguchi, R., Shimizu, T., 2006. Cloning and characterization of mouse lung-type acyl-

CoA:lysophosphatidylcholine acyltransferase 1 (LPCAT1). Expression in alveolar type II cells and possible involvement in surfactant production. J Biol Chem 281, 20140-20147.

Rawlins, E.L., Clark, C.P., Xue, Y., Hogan, B.L., 2009a. The Id2+ distal tip lung epithelium contains individual multipotent embryonic progenitor cells. Development 136, 3741-3745.

Rawlins, E.L., Okubo, T., Xue, Y., Brass, D.M., Auten, R.L., Hasegawa, H., Wang, F., Hogan, B.L., 2009b. The role of Scgb1a1+ Clara cells in the long-term maintenance and repair of lung airway, but not alveolar, epithelium. Cell stem cell 4, 525-534.

Roos, A.B., Berg, T., Barton, J.L., Didon, L., Nord, M., 2012. Airway epithelial cell differentiation during lung organogenesis requires C/EBPalpha and C/EBPbeta. Dev Dyn 241, 911-923.

Schneider, C.A., Rasband, W.S., Eliceiri, K.W., 2012. NIH Image to ImageJ: 25 years of image analysis. Nature methods 9, 671-675.

Shannon, J.M., 1994. Induction of alveolar type II cell differentiation in fetal tracheal epithelium by grafted distal lung mesenchyme. Dev Biol 166, 600-614.

Shannon, J.M., Nielsen, L.D., Gebb, S.A., Randell, S.H., 1998. Mesenchyme specifies epithelial differentiation in reciprocal recombinants of embryonic lung and trachea. Dev Dyn 212, 482-494.

Shin, H.Y., Reich, N.C., 2013. Dynamic trafficking of STAT5 depends on an unconventional nuclear localization signal. J Cell Sci 126, 3333-3343.

Short, K., Hodson, M., Smyth, I., 2013. Spatial mapping and quantification of developmental branching morphogenesis. Development 140, 471-478.

Tadokoro, T., Wang, Y., Barak, L.S., Bai, Y., Randell, S.H., Hogan, B.L., 2014. IL-6/STAT3 promotes regeneration of airway ciliated cells from basal stem cells. Proc Natl Acad Sci U S A 111, E3641-3649.

Treutlein, B., Brownfield, D.G., Wu, A.R., Neff, N.F., Mantalas, G.L., Espinoza, F.H., Desai, T.J., Krasnow, M.A., Quake, S.R., 2014. Reconstructing lineage hierarchies of the distal lung epithelium using single-cell RNA-seq. Nature 509, 371-375.

Wuenschell, C.W., Sunday, M.E., Singh, G., Minoo, P., Slavkin, H.C., Warburton, D., 1996. Embryonic mouse lung epithelial progenitor cells co-express immunohistochemical markers of diverse mature cell lineages. J Histochem Cytochem 44, 113-123.

Xu, B., Qu, X., Gu, S., Doughman, Y.Q., Watanabe, M., Dunwoodie, S.L., Yang, Y.C., 2008a. Cited2 is required for fetal lung maturation. Dev Biol 317, 95-105.

Xu, Q., Tam, M., Anderson, S.A., 2008b. Fate mapping Nkx2.1-lineage cells in the mouse telencephalon. J Comp Neurol 506, 16-29.

Zhou, Q., Brown, J., Kanarek, A., Rajagopal, J., Melton, D.A., 2008. In vivo reprogramming of adult pancreatic exocrine cells to beta-cells. Nature 455, 627-632.

## Figures

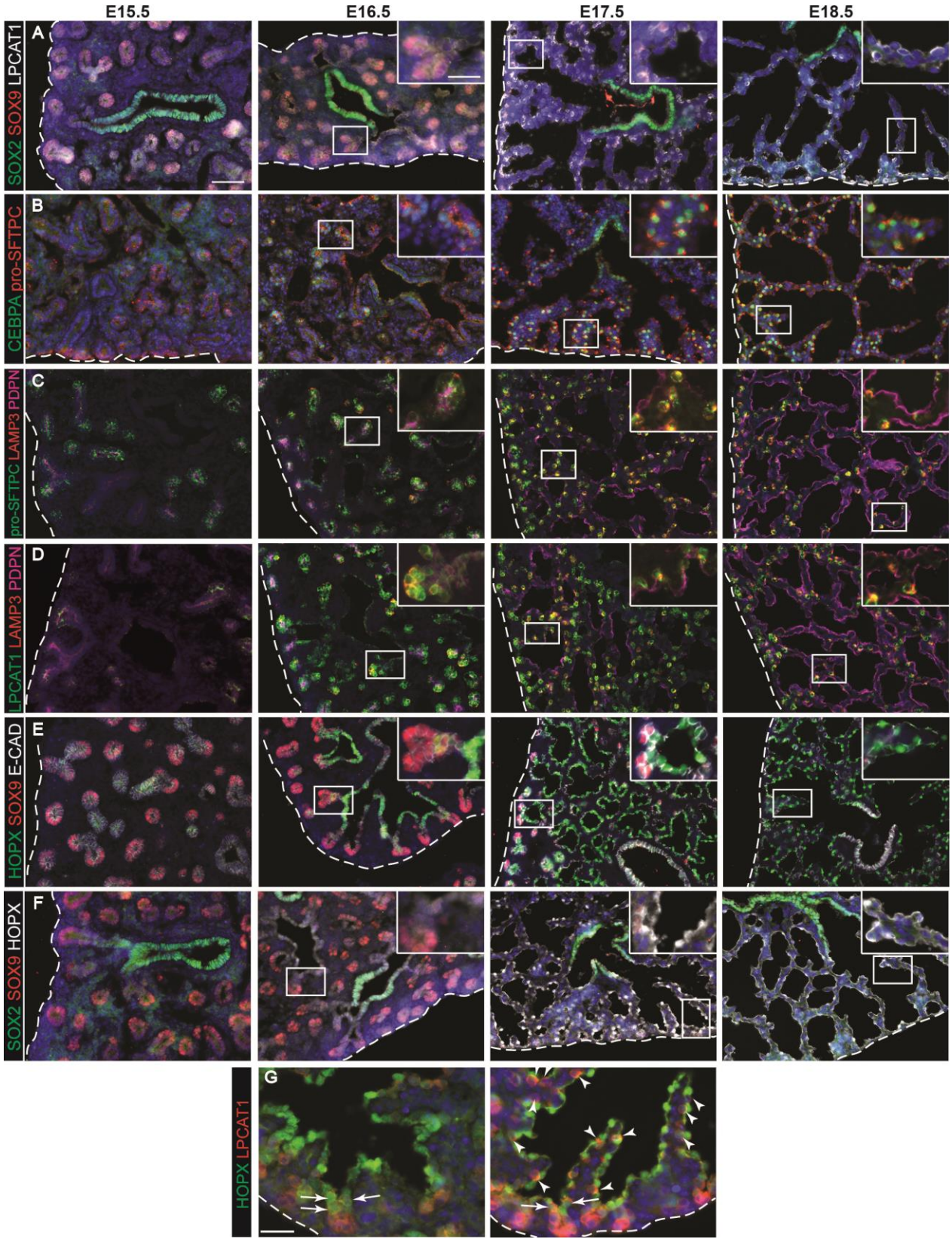

**Figure 1. Evolution of alveolar epithelial gene expression patterns in the developing mouse lung.** Sections of E15.5, 16.5, 17.5 and 18.5 wild-type mouse lungs. A. Green: SOX2 (differentiating bronchioles); red: SOX9 (tips) ; white: LPCAT1 (tip cells from E16.5, then AT2 cells). B. Green: CEBPA (sub-set of tip cells from E16.5, then AT2 cells); red: pro-SFTPC (embryonic epithelium, stronger from E16.5, later specific to AT2 cells). C. Green: pro-SFTPC (stronger from E16.5, later specific to AT2 cells); red: LAMP3 (rare tip cells; AT2 cells); magenta: PDPN (tip cells from E16.5, then AT1 cells). D. green: LPCAT1 (tip cells from E16.5, then AT2 cells); red: LAMP3 (rare tip cells; AT2 cells); magenta: PDPN (tip cells from E16.5, then AT1 cells). E. Green: HOPX (stalk cells from E16.5, AT1 cells); red: SOX9 (tip cells); white: E-CAD (epithelial cells). F. Green: SOX2 (differentiating bronchioles); red: SOX9 (tips) ; white: HOPX (stalk cells from E16.5, AT1 cells). G. Green: HOPX (stalk cells from E16.5, AT1 cells); red: LPCAT1 (tip cells from E16.5, then AT2 cells). Arrows = $LPCAT1^{+}$, $HOPX^{+}$ cells. Arrowheads = $LPCAT1^{+}$, $HOPX^{-}$ cells. Blue: DAPI (nuclei). Dashed line = edge of lung. Bars = 50 μm A-F; 20 μm G and insets.

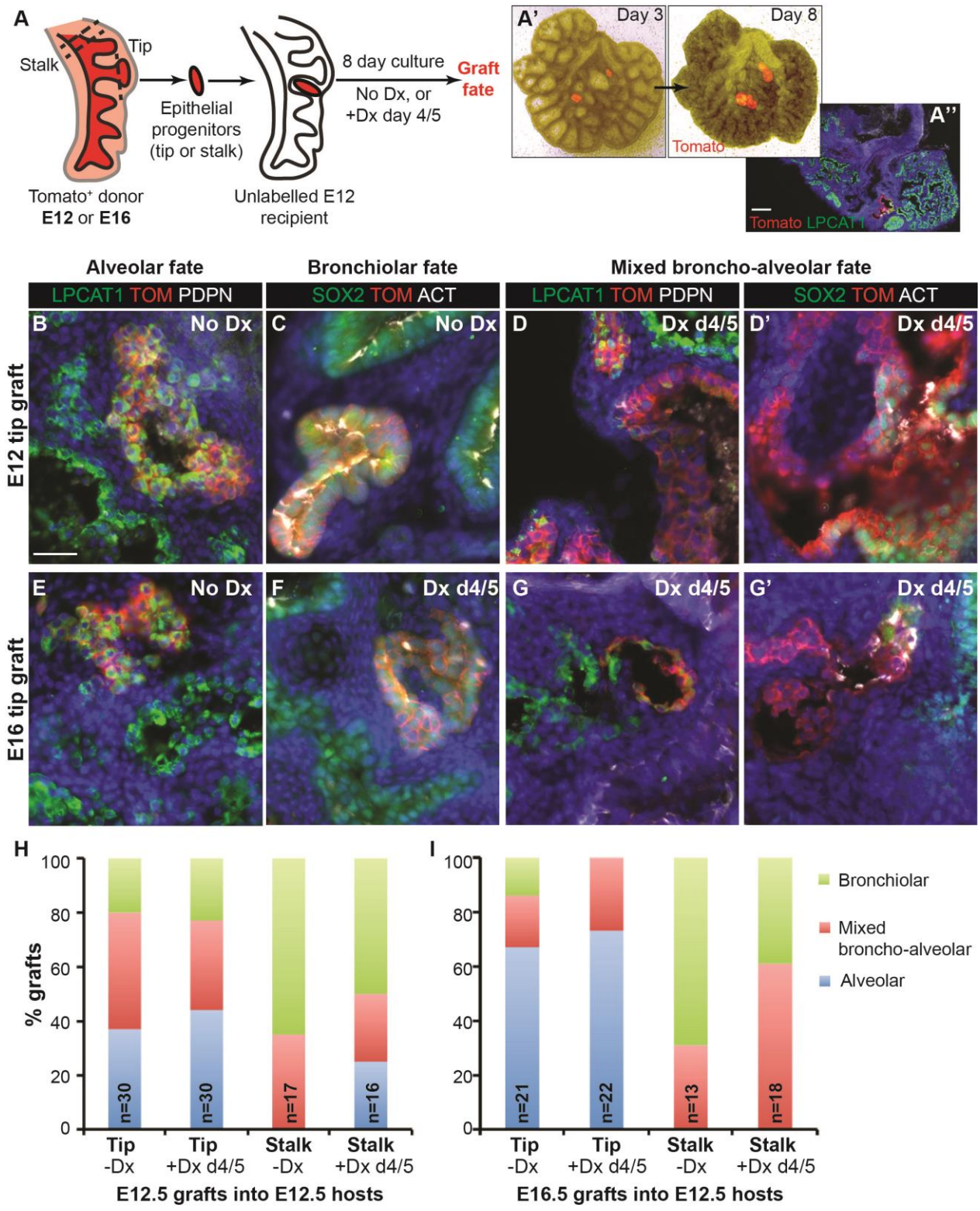


**Figure 2. Extrinsic factors are the major determinant of progenitor cell identity in the developing mouse lung.** A. Experimental outline. Epithelial progenitors (tip or stalk) were microdissected from donor E12.5 or E16.5 Tomato$^{+}$ (*Rosa26R*$^{mT\text{-}mG/+}$) lungs and grafted into the mesenchyme of unlabelled E12.5 hosts. Hosts/grafts were cultured for 8 days without Dx, or with addition of 50 nM Dx at culture day 4 /5, followed by serial sectioning and staining to determine

graft fate. A',A''. Grafts integrate into the host lung, grow and form a lumen. B-G. Sections of grafted lungs with alternate slides stained for green: LPCAT1 (alveolar fate); red: Tomato (graft); white: PDPN (basal and AT1 cells), or green: SOX2 (bronchiolar fate); RFP (graft); white: acetylated tubulin (cilia) to determine graft fate. Examples of tip grafts with alveolar, bronchiolar and mixed broncho-alveolar fate are shown. Note D/D' and G/G' are different sections of the same graft. H, I. Quantitation of graft fate/numbers of grafts analysed. Each type of graft was analysed in at least three independent experiments. Bars = 25 μm A''; 100 μm B-G.

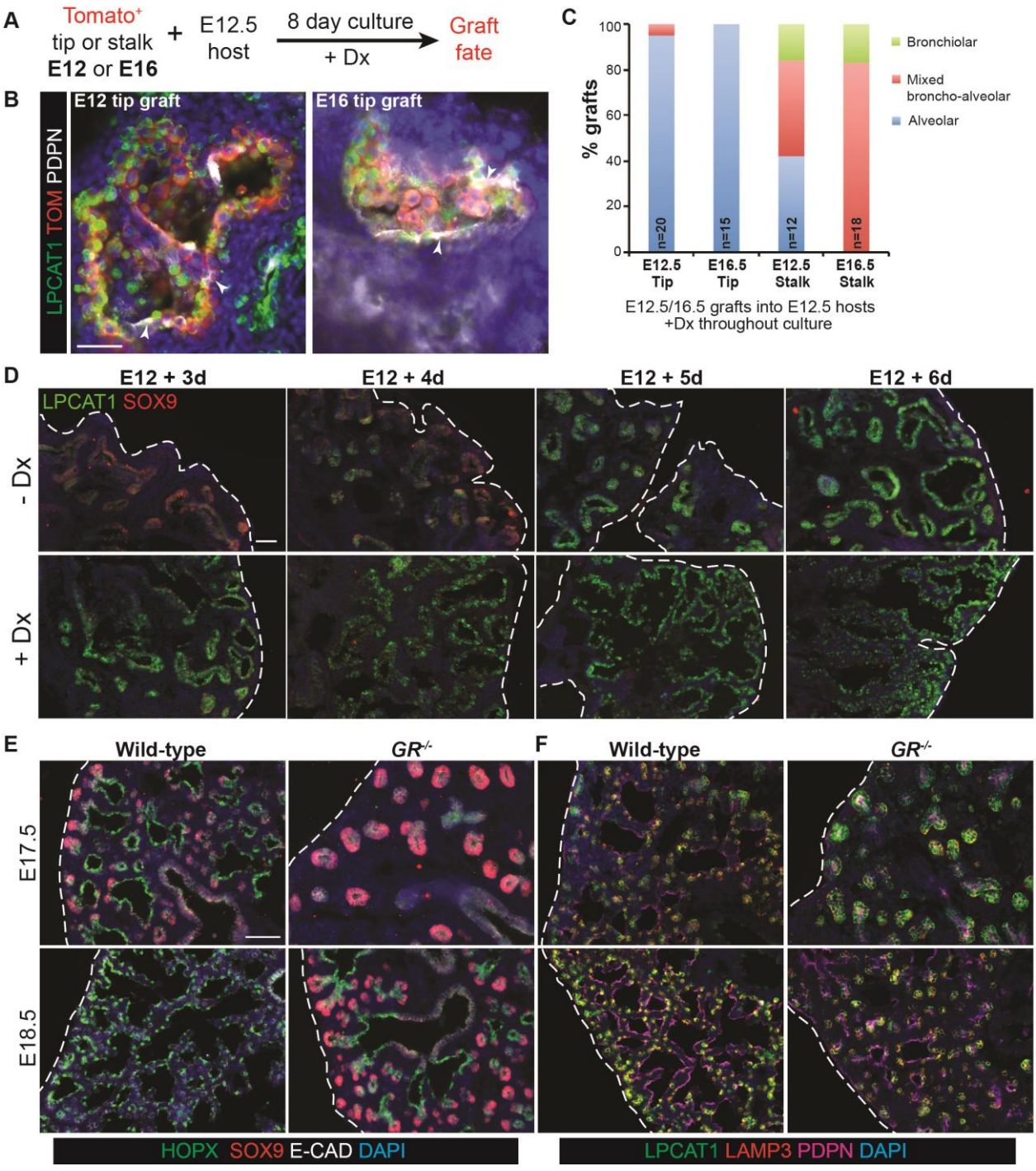


**Figure 3. Glucocorticoid signalling is sufficient, but not essential, to specify alveolar fate.** A. Experimental design: Tomato$^{+}$ E12.5 or 16.5 tip or stalk was grafted into E12.5 host lung and grown with 50 nM Dx throughout culture. B. Examples of alveolar-fated tip grafts stained for green: LPCAT1 (alveolar fate); red: Tomato (graft); white: PDPN (basal and AT1 cells). Arrowheads = PDPN$^{+}$ AT1 cells. C. Split bar graph showing results from B. Each type of graft was analysed in at least three independent experiments. D. E12.5 wild-type lungs were grown with, or without, Dx for up to 6 days; 2 independent experimental replicates. Note precocious expression of alveolar markers in the presence of Dx. Lungs cultured without Dx do express

LPCAT1 from experimental day 5. Green: LPCAT1 (late tip progenitors and type 2 cells); red: SOX9 (tip progenitors). E, F. Sections of *GR*$^{-/-}$ and *GR*$^{+/+}$ sibling lungs at E17.5 and E18.5 stained for green: HOPX (AT1 cells); red: SOX9 (tip progenitors); white: E-CAD (epithelium) (E), and green: LPCAT1 (late tip progenitors and AT2 cells); red: LAMP3 (AT2 cells); magenta: PDPN (late tip progenitors and AT1 cells) (F). A total of 5 *GR*$^{-/-}$ and 5 *GR*$^{+/+}$ sibling lungs from 3 independent litters were observed at both E17.5 and E18.5. Blue: DAPI. Bars = 100 μm B; 50 μm D-F.

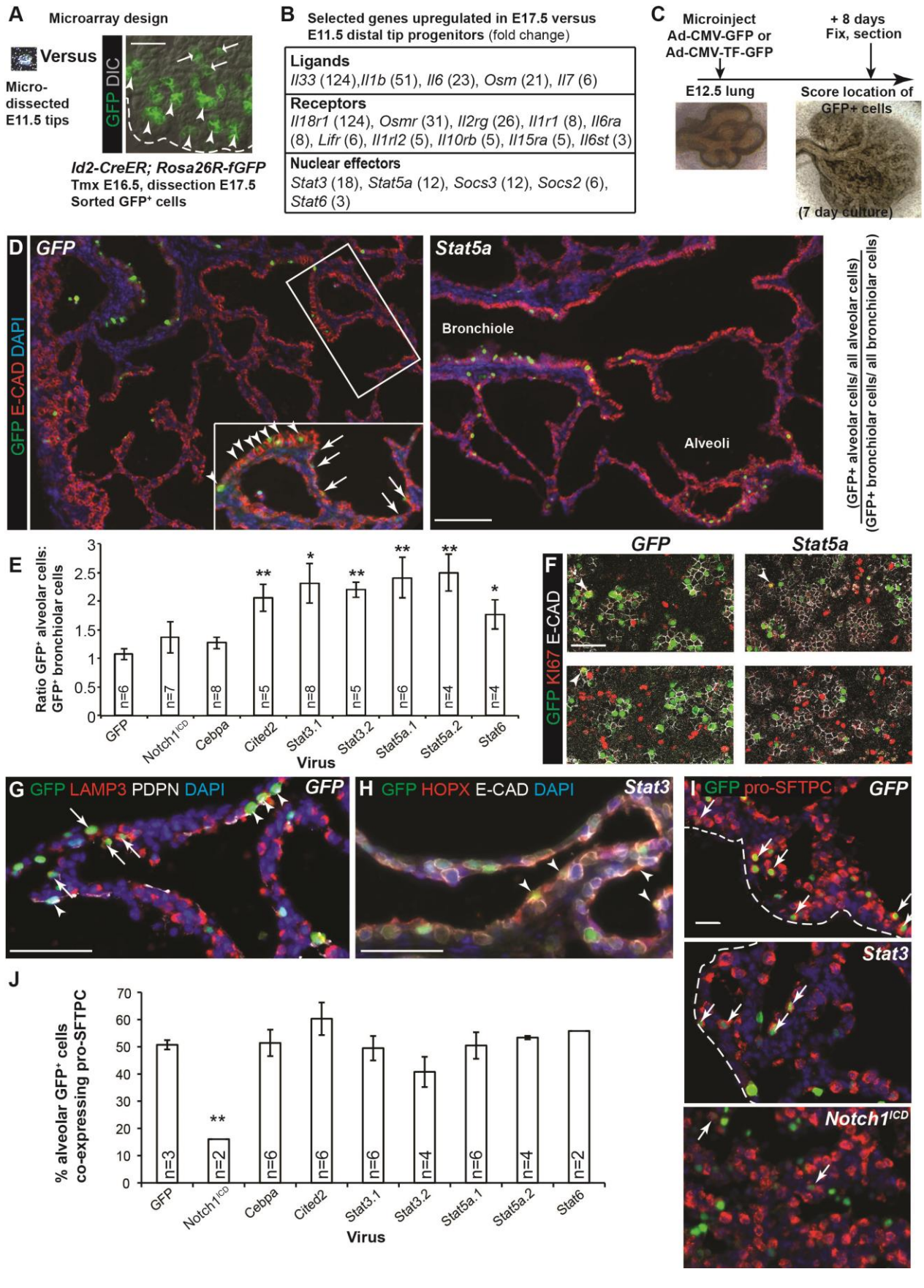

**Figure 4**. **Overexpression of *Stat* genes promotes alveolar fate in distal tip progenitor cells.** A. RNA was extracted from microdissected E11.5 distal tips. And from flow-sorted $GFP^+$ E17.5 tip progenitors (arrowheads), and their immediate alveolar-fated progeny (arrows), from *Id2-CreER; Rosa26R-fGFP* embryos lineage-labelled by tmx injection at E16.5. B. Selected genes upregulated in E17.5 versus E11.5 samples. Fold change is shown in brackets. C. Experimental design for adenoviral-mediated overexpression of TFs in E12.5 lung epithelium. D. Representative images of *GFP* control and *Stat5a* adenoviral-infected lungs. Green: GFP (transduced cells); red: E-CAD (epithelium). All $GFP^+$ and all $E\text{-}CAD^+$ cells were counted manually. Bonchiolar (arrowheads) versus alveolar (arrows) fate was based on the location, morphology (columnar or squamous) and intensity of the E-CAD staining. E. Quantification of the ratio of $GFP^+$ alveolar: $GFP^+$ bronchiolar cells normalised to the total numbers of alveolar and bronchiolar epithelial cells scored. F. Sections of adenovirus-transduced lungs. Green: GFP (transduced cells); red: KI67 (proliferating cells); white (E-CAD) epithelium. Arrowheads = proliferating $GFP^+$ epithelial cells. G. Green: GFP (transduced cells); red: LAMP3 (AT2); white: PDPN (AT1). Arrows = $GFP^+$ AT2 cells. Arrowheads = $GFP^+$ AT1 cells. H. Green: GFP (transduced cells); red: HOPX (AT1); white: E-CAD (epithelium). Arrowheads = $GFP^+$ AT1 cells. I. Green: GFP (transduced cells); red: pro-SFTPC (AT2 cells). Arrows = co-expressing cells scored as $(GFP, \text{pro-SFTPC})^+$. J. Quantification of the percentage of alveolar $GFP^+$ cells which co-express pro-SFTPC. Blue: DAPI (nuclei). Bars = 100 μm A,D; 50 μm E,G-I. Error bars represent s.e.m. * $p<0.05$; ** $p<0.01$. Full experimental details are presented in the accompanying raw data table supplement.

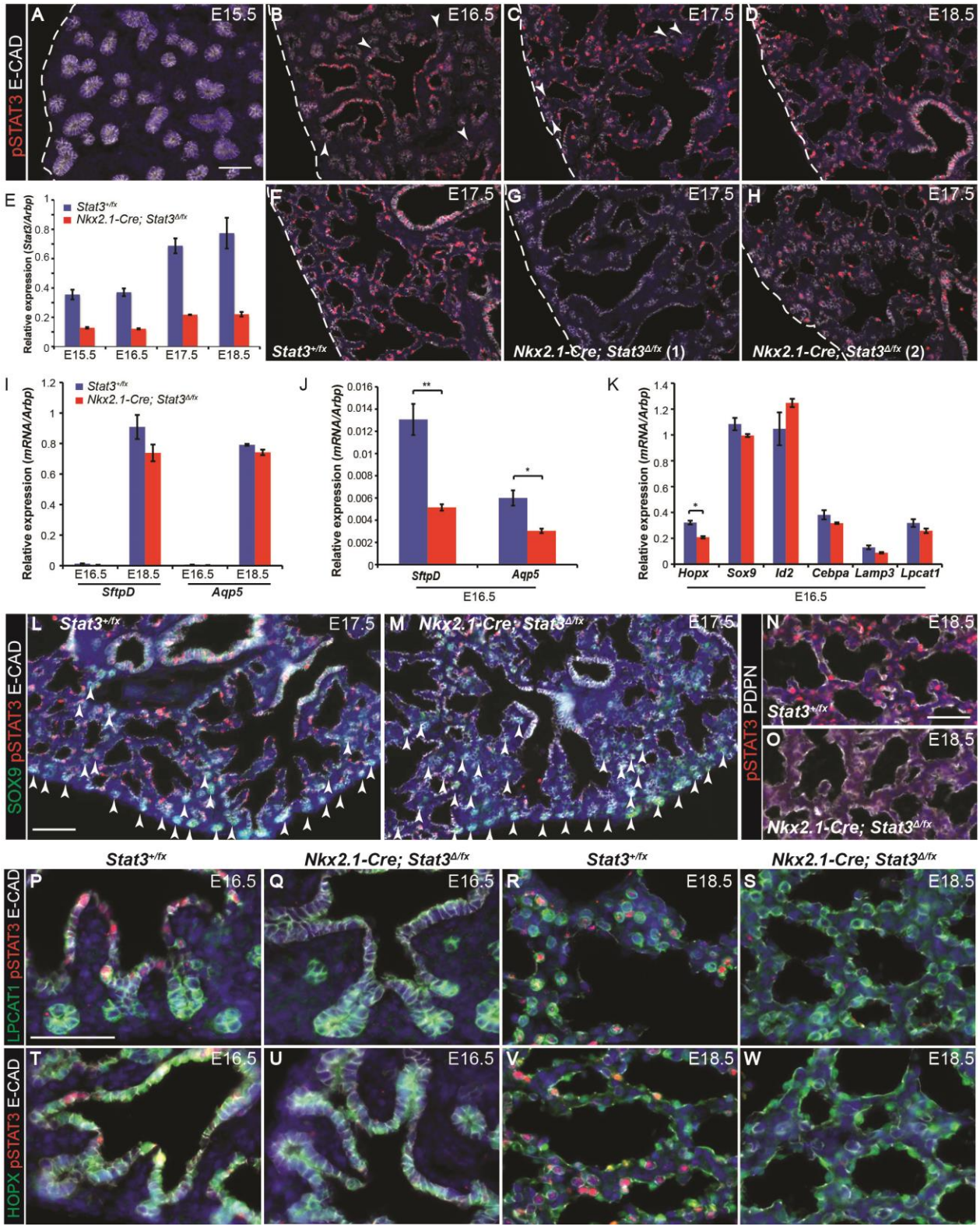


**Figure 5. Lung epithelial specific knock-out of *Stat3* results in a brief delay in lung development.** A-D. Sections of E15.5, 16.5, 17.5 and 18.5 wild-type mouse lungs stained to show phosphorylated (active) STAT3 protein. Red: pSTAT3; white: E-CAD (epithelium). E. RT-qPCR for *Stat3* in *Nkx2.1-Cre; Stat3*$^{\Delta/fx}$ and sibling *Stat3*$^{fx/+}$ lungs. 5 lungs of each genotype were collected from 3 independent litters. F-H. pSTAT3 staining in sibling control (F) and cKO (G, H)

lungs shows the highly variable extent of recombination. Red: pSTAT3; white: E-CAD (epithelium). I-K. RT-qPCR from *Nkx2.1-Cre; Stat3*$^{\Delta/fx}$ and sibling *Stat3*$^{fx/+}$ lungs. I, J. Mature differentiation markers *SftpD* and *Aqp5* at E16.5 and E18.5. K. Late progenitor/early differentiation markers at E16.5. L-W. Sections of *Stat3* cKO and sibling lungs. L,M. E17.5. Green: SOX9 (tip progenitors); red: pSTAT3; white: E-CAD (epithelium). N,O. E18.5. Red: pSTAT3; white: PDPN (type 1 cells). P-S. Green: LPCAT1 (late tip progenitors and type 2 cells); red: pSTAT3; white: E-CAD (epithelium) at E16.5 (P, Q) and E18.5 (R, S). T-W. Green: HOPX (type 1 cells); red: pSTAT3; white: E-CAD (epithelium) at E16.5 (T, U) and E18.5 (V, W). Blue: DAPI. Bars = 50 μm, except 100 μm L,M. Error bars = s.e.m. * $p<0.05$; ** $p<0.01$

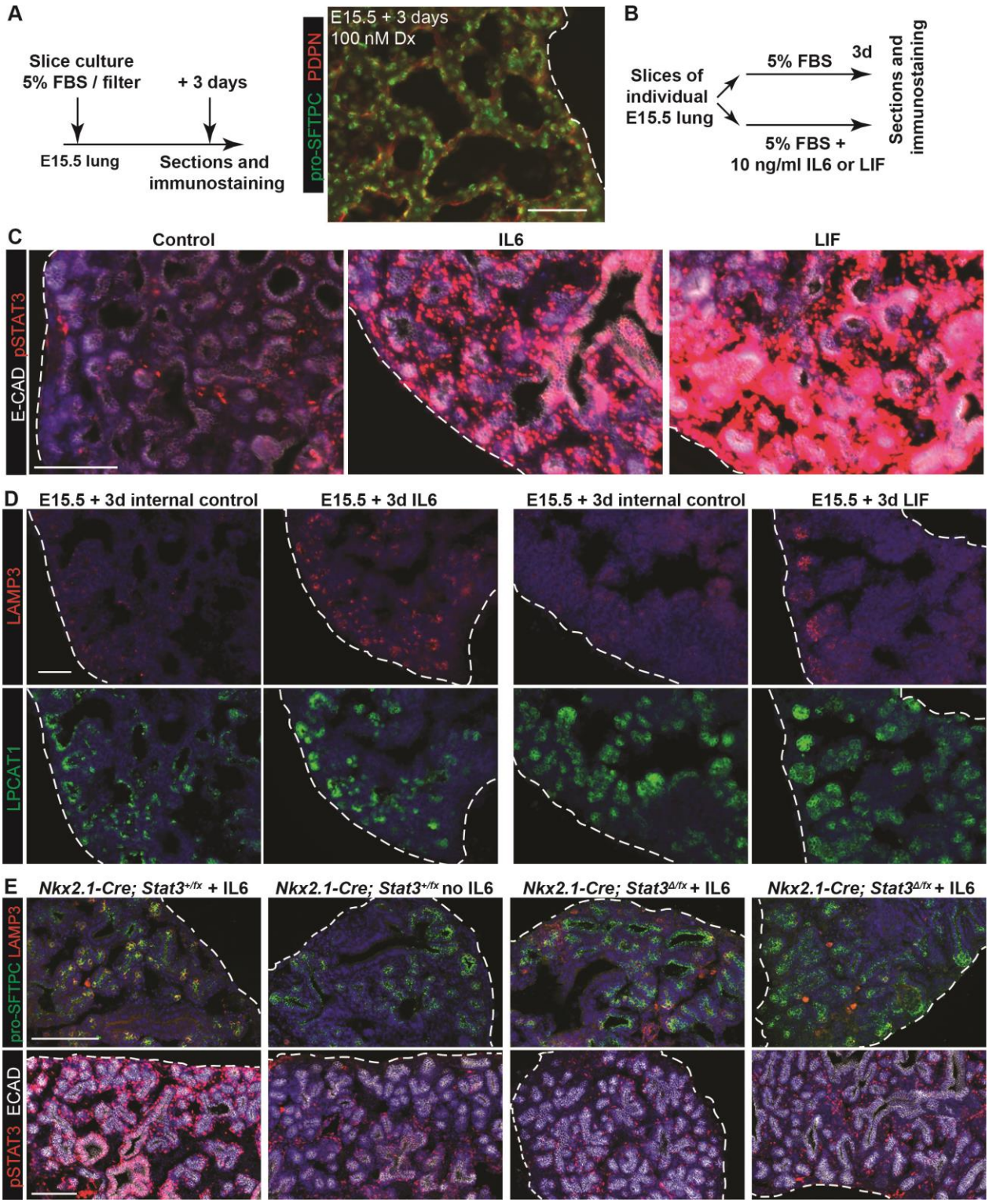


**Figure 6. Ectopic IL6 family ligands result in accelerated AT2 differentiation via STAT3 activation.** A. Schematic and section of E15.5 slice culture resulting in differentiation of mature saccules with AT1 and 2 cells in the presence of Dx. Green: pro-SFTPC; red: PDPN. B. Schematic of IL6 and LIF experiments. Slices from individual lungs were split between two conditions for internal controls. C,D. Sections from control, IL6 and LIF-exposed wild-type lungs. C. Red: pSTAT3; white: E-CAD (epithelium). D. Red: LAMP3 (differentiating AT2 cells); green

LPCAT1 (late tip and AT2 cells). E. Sections from control (*Nkx2.1-Cre; Stat3*$^{+/fx}$) and mutant (*Nkx2.1-Cre; Stat3*$^{\Delta/fx}$) lungs +/- IL6. (N=9 *Nkx2.1-Cre; Stat3*$^{\Delta/fx}$ lungs analysed in 3 independent experiments.) Top panels: green: pro-SFTPC; red: LAMP3. Lower panels: red: pSTAT3; white: E-CAD (epithelium). Blue: DAPI. Bars = 50 μm A,D; 100 μm C,E.

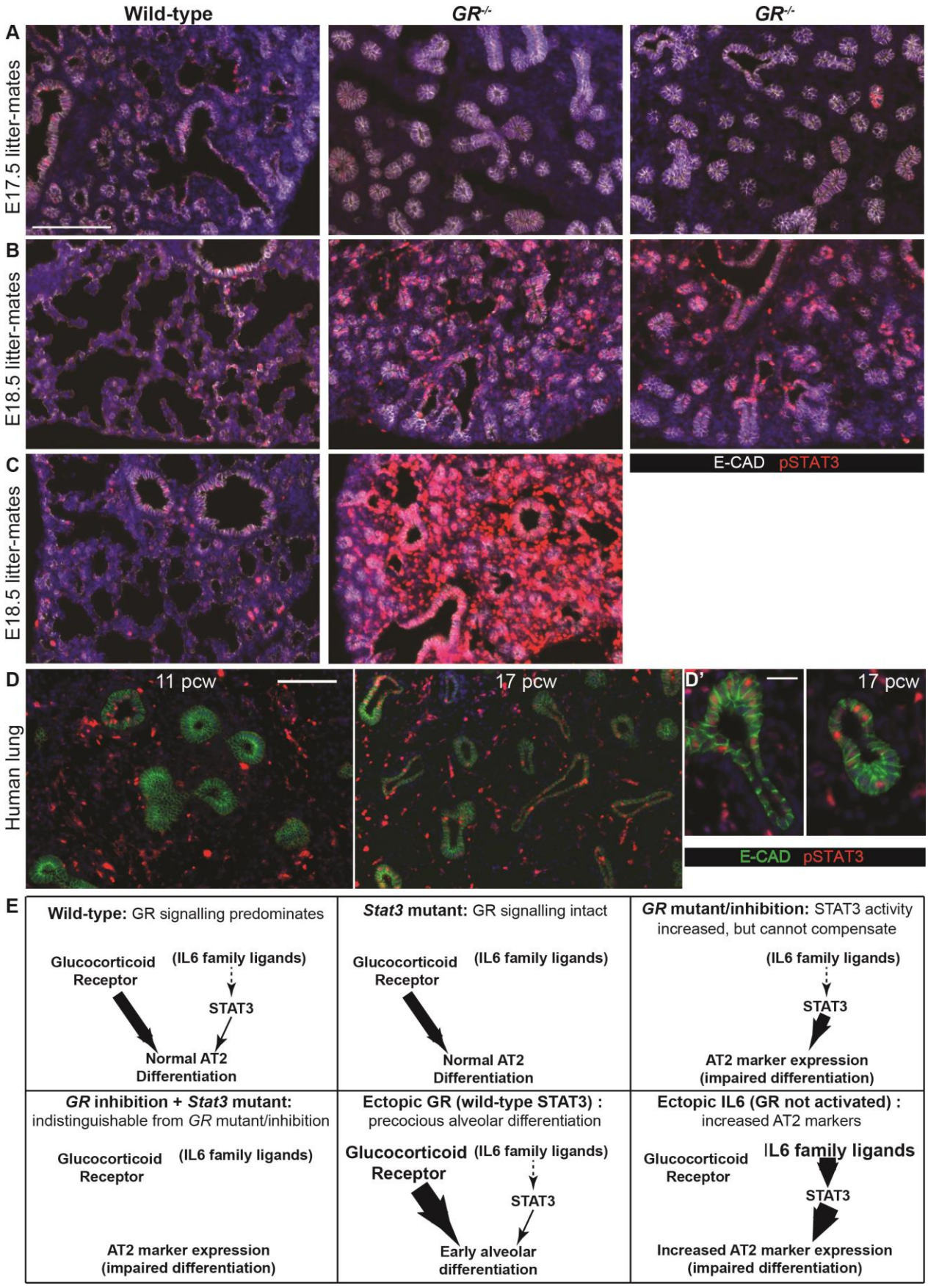

**Figure 7. STAT3 and glucocorticoid function co-operatively in alveolar differentiation.** A-C. Cryosections of *GR*$^{-/-}$ and littermate lungs. Red: pSTAT3; white: E-CAD. A. E17.5 littermates. B. E18.5 littermates. C. Independent E18.5 littermates. A total of 5 *GR*$^{-/-}$ and 5 *GR*$^{+/+}$ sibling lungs from 3 independent litters were observed at both E17.5 and E18.5. D. Human embryonic lung sections from 11 and 17 pcw. Green: E-CAD (epithelium); Red: pSTAT3; blue: Dapi. Note the presence of mesenchymal background staining in the 11 and 17 pcw human samples. E. We propose that in wild-type lung development STAT3 and GR signalling work in parallel to promote alveolar differentiation. GR has the predominant role indicated by subtle phenotypes in the *Stat3* mutant and impaired differentiation, but only slightly delayed alveolar specification, in the *GR* mutant. Loss of both pathways does not result in a greater phenotype, indicating that the ectopic pSTAT3 observed in the *GR* mutants is not sufficient to compensate. Nevertheless, ectopic activation of either pathway is sufficient to promote aspects of alveolar differentiation with the exact effects depending on timing. However, given that neither pathway is absolutely necessary for the initiation of alveolar differentiation to occur, other signalling mechanisms must also be involved. Bar = 100 μm A-D; 20 μm D'.

## SUPPLEMENTAL FIGURES

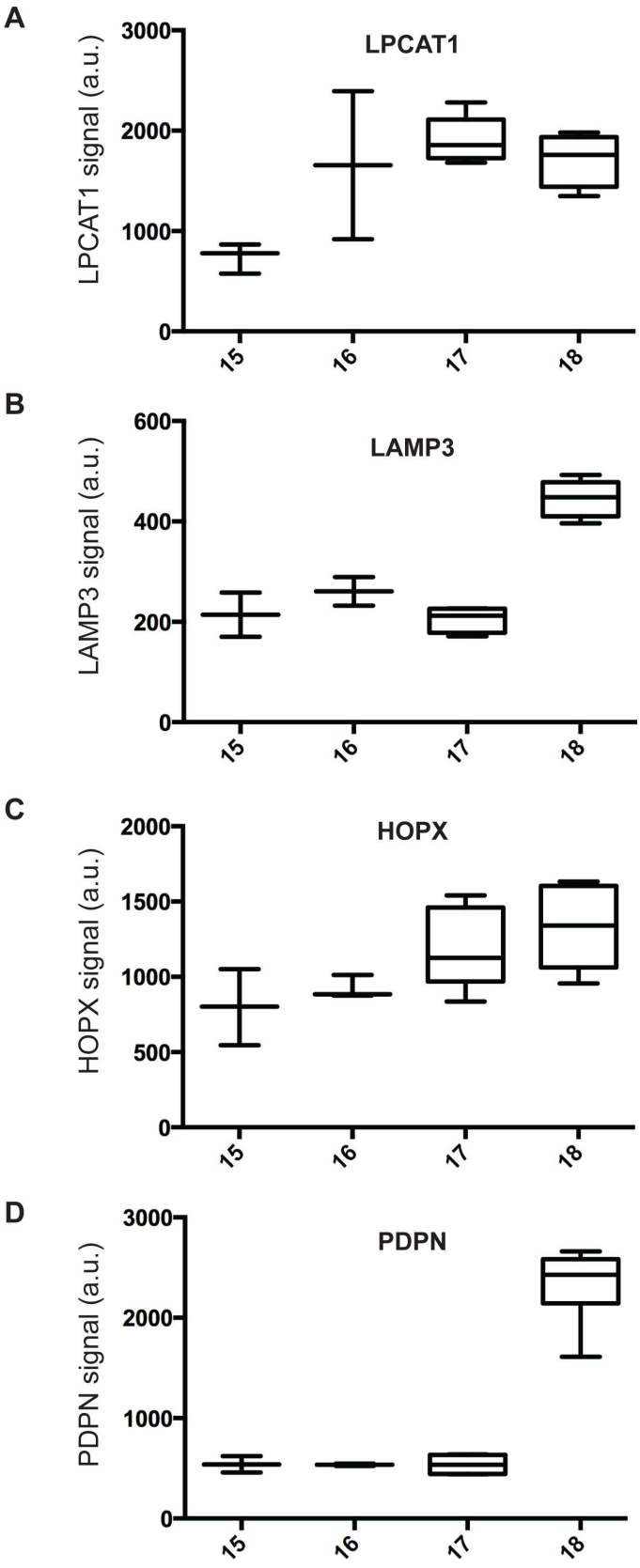

**Figure S1. Relative expression level of alveolar epithelial fate markers in normal lung development over time.** Bar and whisker plots showing relative expression levels of alveolar fate markers analysed in Figure 1 in arbitrary units normalized to the total cell area sampled. A. LPCAT1 (raw data from images underpinning Fig. 1D). B. LAMP3 (raw data from images underpinning Fig 1D). C. HOPX (raw data from images underpinning Fig. 1F). D. PDPN (raw data from images underpinning Fig. 1D).

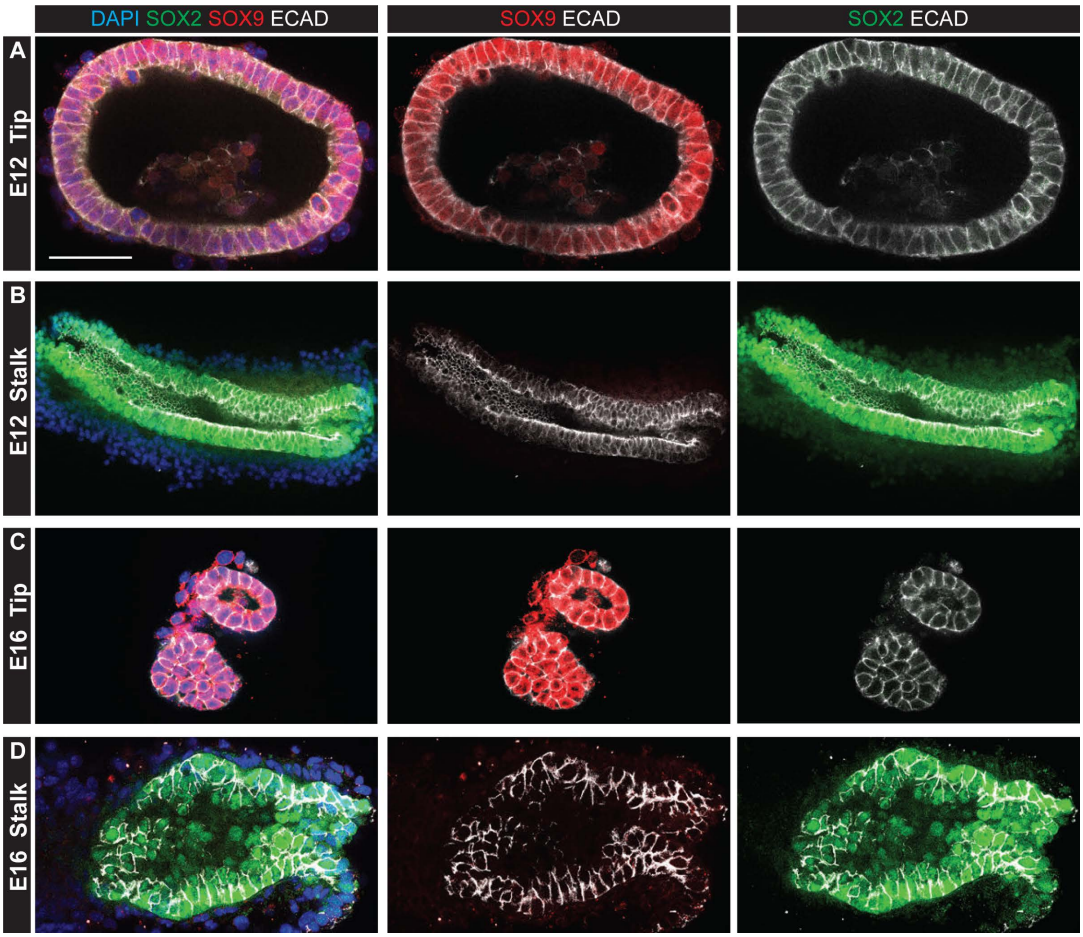


**Figure S2. Microdissected tip and stalk cells.** Examples of wholemount stained microdissected tip and stalk cells. Green: SOX2 (stalk/differentiating bronchioles); red: SOX9 (tip); white: E-CAD (epithelium); blue: DAPI (nuclei). A. E12.5 tip. B. E12.5 stalk. C. E16.5 tip. D. E16.5 stalk. Bars = 50 μm A,C,D; 100 μm B.

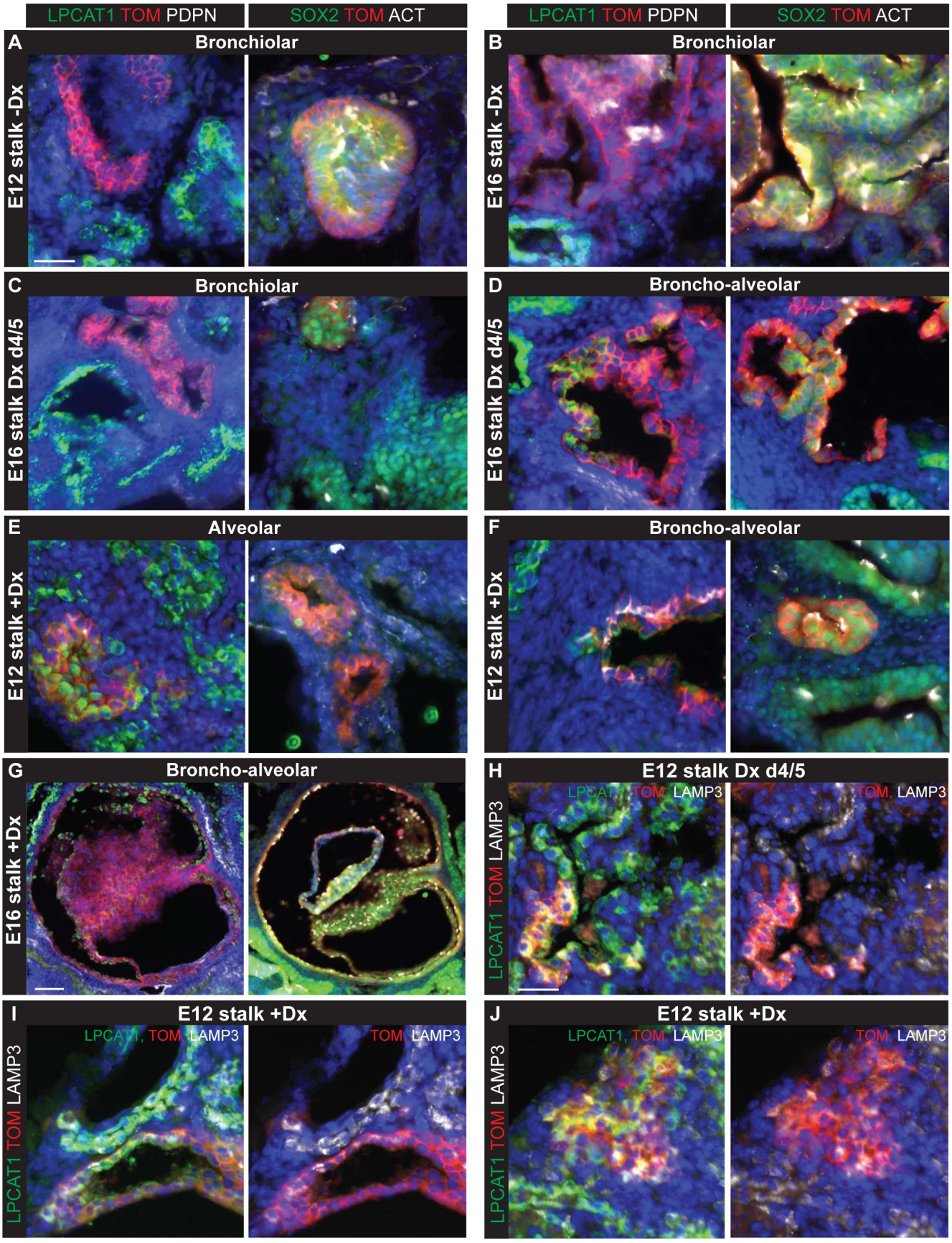

**Figure S3. Grafted stalk cells can respond to the host environment and alter progeny cell fate.** Examples of grafted stalk cells following 8 days of culture in various conditions. A-G. Two images of each graft are shown taken from adjacent slides stained to detect alveolar fate: green: LPCAT1 (alveolar fate); red: Tomato fluorescence (grafted cells); white: PDPN (basal and type 1 cells), or bronchiolar fate: green: SOX2 (bronchiolar fate); red: RFP (Tomato$^{+}$ graft); white: acetylated tubulin (cilia) to determine graft fate. A. E12.5 stalk, no Dx, bronchiolar-fated. B. E16.5 stalk, no Dx, bronchiolar-fated. C. E16.5 stalk, Dx day4/5, bronchiolar fated. D. E16.5 stalk, Dx day4/5, mixed broncho-alveolar fated. E. E12.5 stalk, Dx throughout, alveolar fated. F. E12.5 stalk, Dx throughout, mixed broncho-alveolar fated. G. E16.5 stalk, Dx throughout, mixed broncho-alveolar fated. H-J. Grafts are stained to detect alveolar markers. Green: LPCAT1 (alveolar fate); red: Tomato fluorescence (grafted cells); white: LAMP3 (differentiating AT2 cells). Right panel has the green channel removed to show the Tomato/LAMP3 co-localisation clearly. H. E12.5 stalk, Dx day4/5. I, J. E12.5 stalk, Dx throughout. Bars = 50 μm C left panel; 100 μm all other panels.

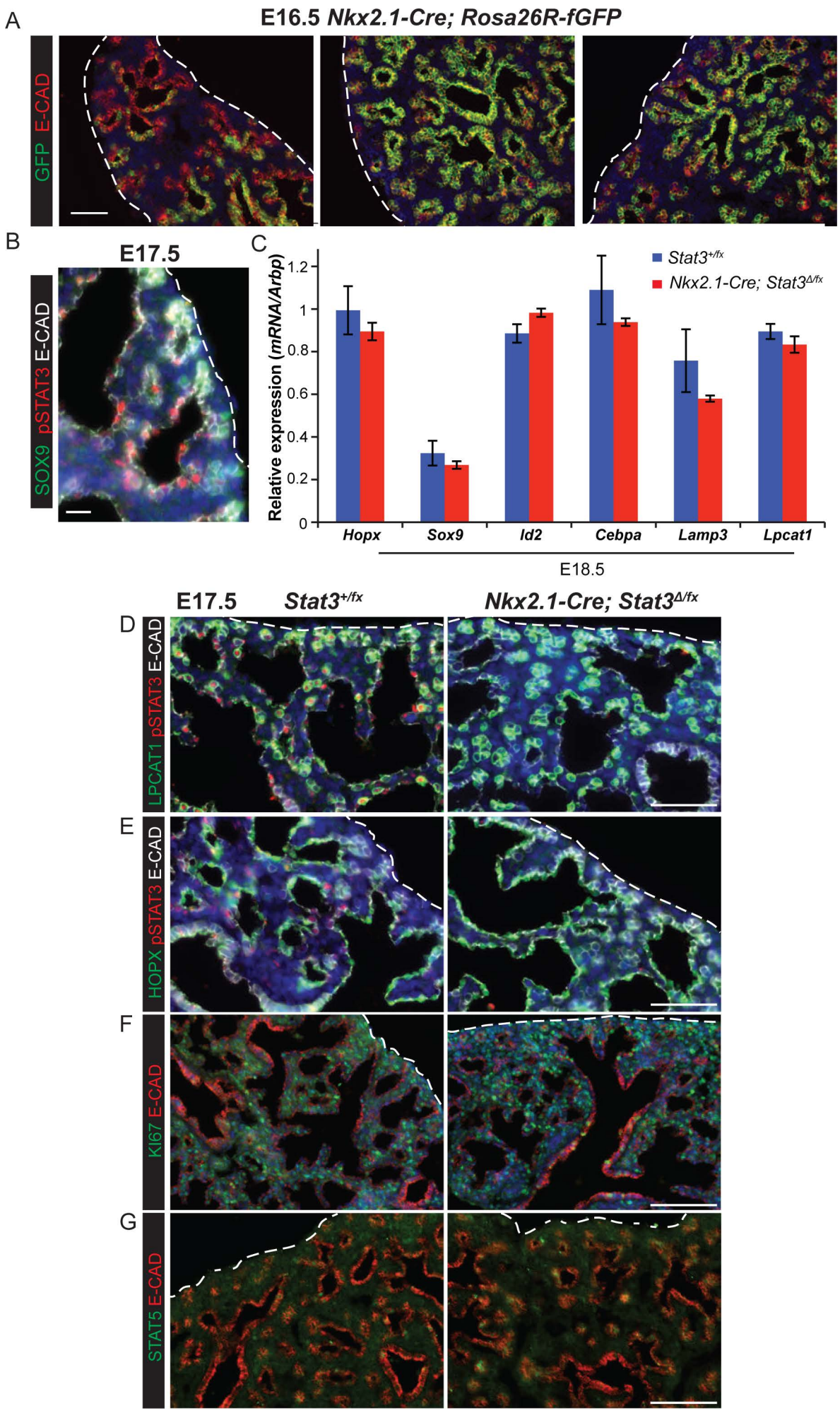

**Figure S4. Alveolar maturation ultimately occurs in the *Stat3* cKO lungs.** A. Sections of E16.5 *Nkx2.1-Cre; Rosa26R-fGFP* lungs illustrating variation in the extent of recombination. Green: eGFP (reporter); red: E-CAD (epithelium). B. Section of E17.5 wild-type lung illustrating that pSTAT3 is predominantly seen in differentiating cells that have exited the tip. Green: SOX9 (tip); red: pSTAT3; white: E-CAD (epithelium). C. RT-qPCR of progenitor and alveolar markers from *Nkx2.1-Cre; Stat3*$^{\Delta/fx}$ and sibling *Stat3*$^{fx/+}$ control E18.5 lungs. Error bars = s.e.m. D, E. Sections of *Stat3* cKO and sibling lungs. D. Green: LPCAT1 (late tip and AT2 cells); red: pSTAT3; white: E-CAD (epithelium). E. Green: HOPX (differentiating AT1 cells); red: pSTAT3; white: E-CAD (epithelium). F: Green: Ki67 (proliferating cells); red: E-CAD (epithelium); blue: Dapi. G. Green: STAT5; red: E-CAD (epithelium). H. Quantification of LPCAT1 and HOPX staining in E17.5 and E18.5 *Nkx2.1-Cre; Stat3*$^{\Delta/fx}$ and sibling *Stat3*$^{fx/+}$ control. Mean and s.e.m. are displayed for 3 independent samples. Bar = 50 µm A, D, E; 25 µm B; 100 µm F, G.

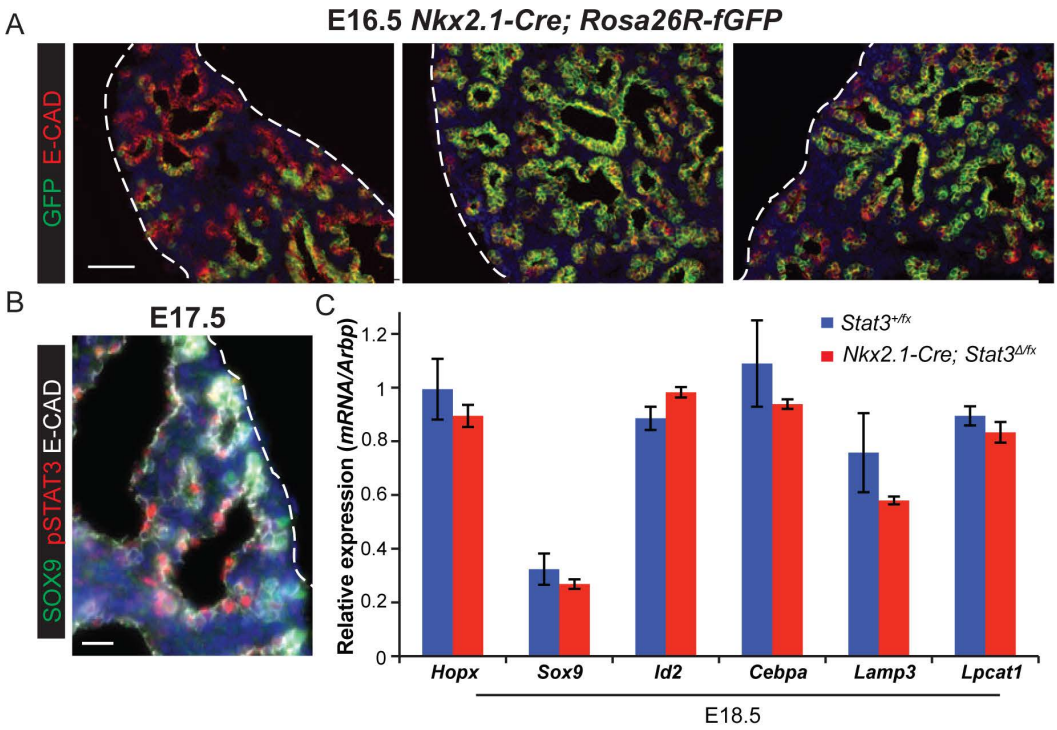


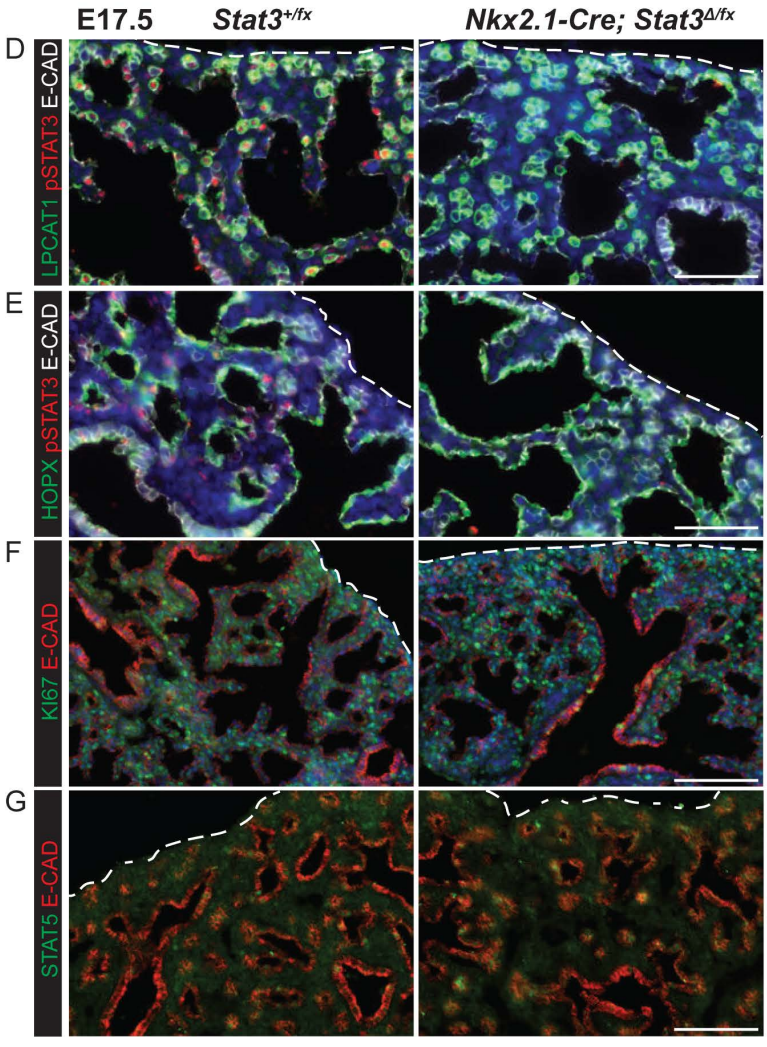


H

**% alveolar epithelial cells expressing LPCAT1**

| | *Stat3*$^{+/fx}$ | *Nkx2.1-Cre; Stat3*$^{\Delta/fx}$ |
|---|---|---|
| E17.5 | 79 +/- 2.3% | 81 +/- 2.2% |
| E18.5 | 70 +/- 0.5% | 71 +/- 2.6% |

**% alveolar epithelial cells expressing HOPX**

| | *Stat3*$^{+/fx}$ | *Nkx2.1-Cre; Stat3*$^{\Delta/fx}$ |
|---|---|---|
| E17.5 | 69 +/- 1.3% | 67 +/- 2% |
| E18.5 | 52 +/- 1.1% | 57 +/- 2.1% |

**Figure S5. Lung epithelial specific knock-out of *Stat5a/b* does not result in alveolar differentiation phenotypes.** A. Wild-type E15.5, 16.5, 17.5 lung sections. Green: E-CAD (epithelium); Red: STAT5A. B. RT-qPCR of *Stat5a* and progenitor/alveolar markers from *Nkx2.1-Cre; Stat5*$^{\Delta/fx}$ and sibling *Stat5*$^{fx/+}$ control lungs. Error bars = s.e.m. C-F. Sections of *Stat5* cKO and sibling control lungs. C. E18.5. Green: LAMP3 (differentiating AT2 cells); red: PDPN (AT1 cells). D. E18.5. Green: LPCAT1 (AT2 cells); red: SOX9 (progenitor cells). E. E18.5. Green: KI67 (proliferating cells); red: E-CAD (epithelium). F. E16.5. Green: E-CAD (epithelium); red: STAT3. At each time-point, three independent litters were collected and stained. Blue: Dapi. Bar = 50 μm A, E, F; 100 μm C,D.

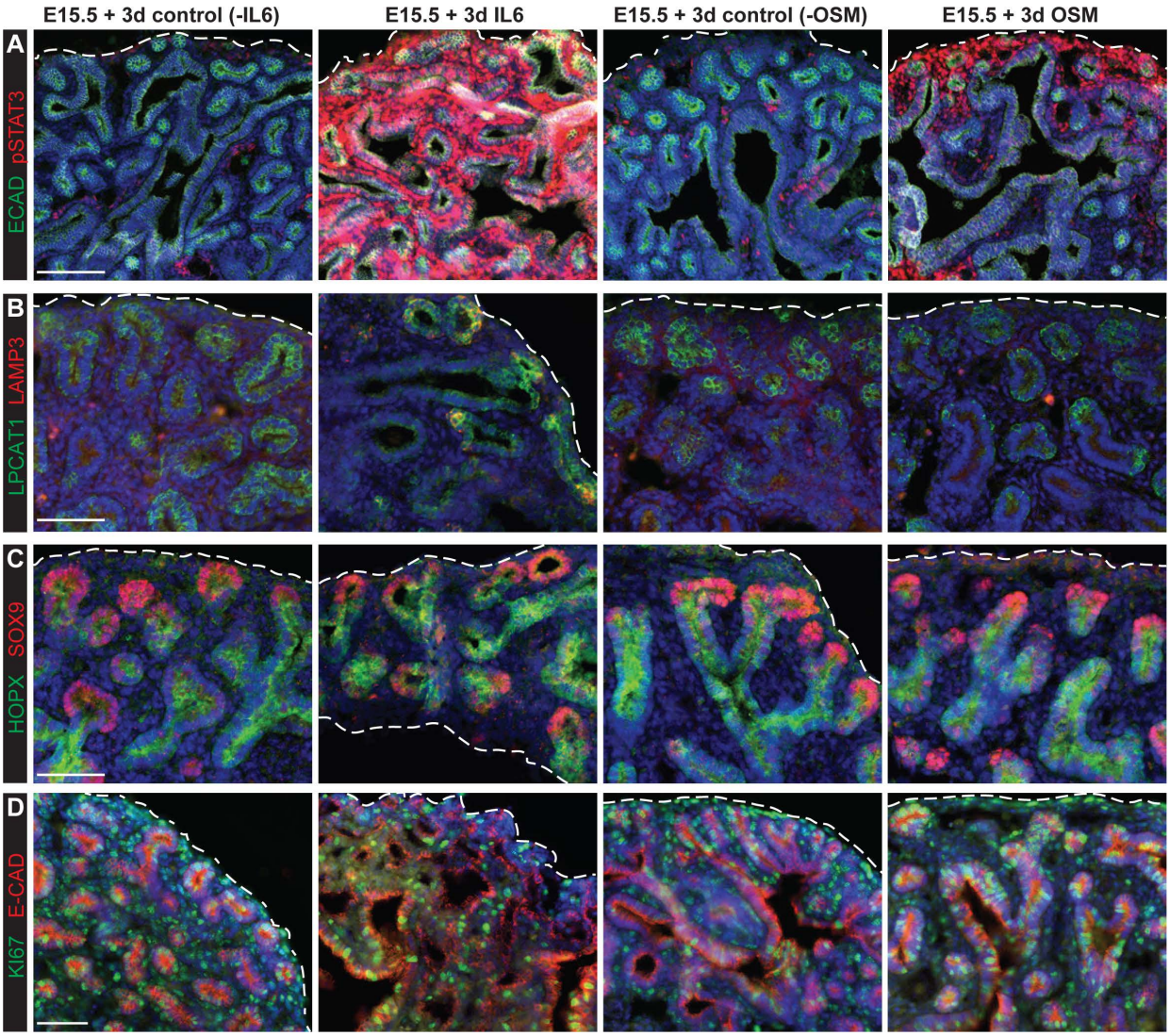


**Figure S6. Activating pSTAT3 via OSM is not sufficient to accelerate AT2 differentiation.** Sections of E15.5 lung slices cultured for 3 days +/- 10 ng/ml IL6, or +/- 25 ng/ml OSM. A. Green: E-CAD (epithelium); red (pSTAT3). B. Green: LPCAT1 (late tip and AT2); red: LAMP3 (AT2). C. Green: HOPX (stalk cells from E16.5, AT1 cells); red: SOX9. D. Green: KI67 (proliferating cells); red: E-CAD (epithelium); Blue: Dapi. Bar = 100 μm A; 50 μm B-D.

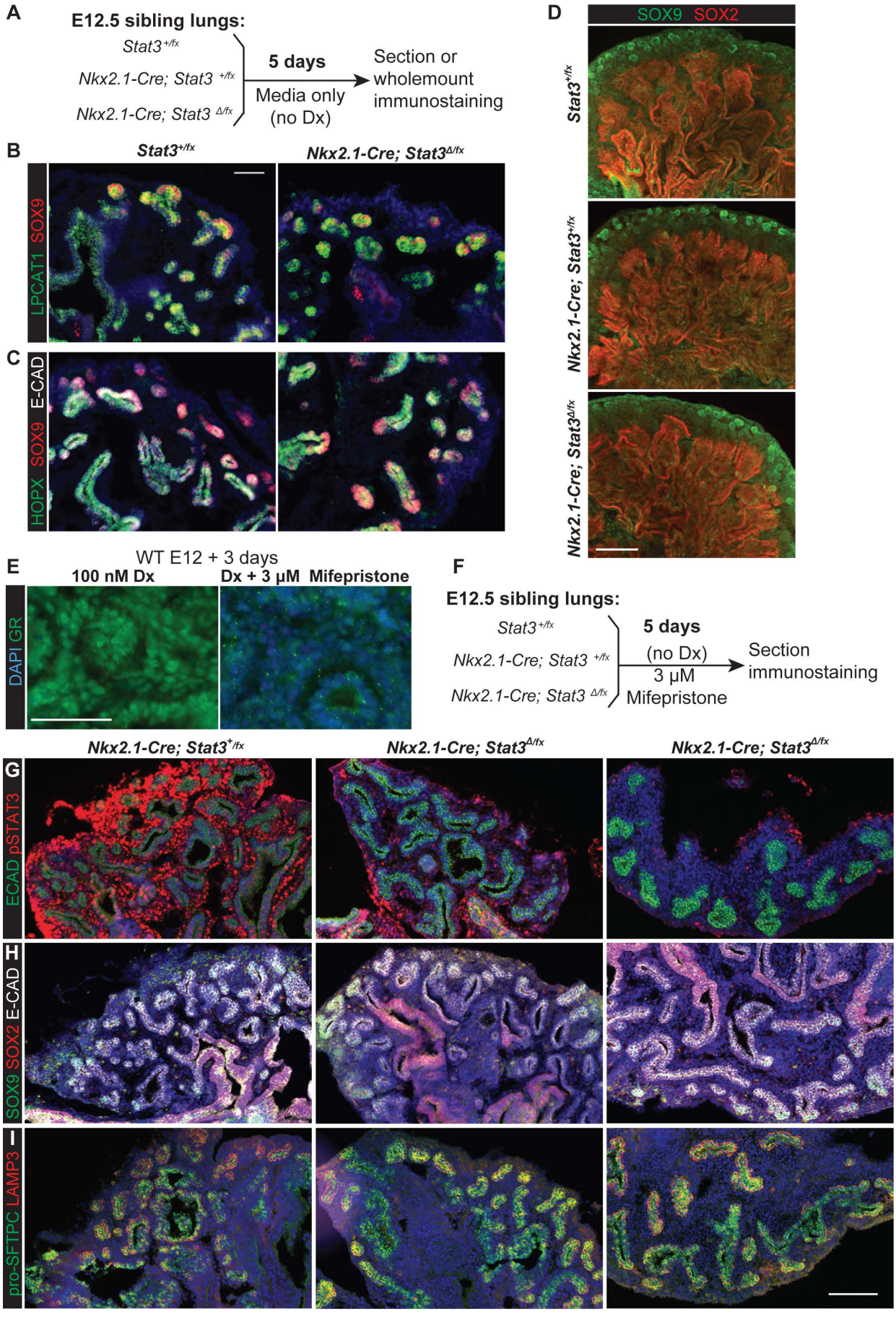

**Figure S7. No evidence for redundant Glucocorticoid and STAT3 activity in alveolar development.** A. Experimental scheme: E12.5 *Stat3* cKO and sibling control lungs were cultured for 5 days in the absence of exogenous glucocorticoid. B, C. E12.5 + 5 day sections (n=6 *Stat3* cKO lungs in two independent experiments). B. Green: LPCAT1; red: SOX9. C. Green: HOPX; red: SOX9; white: E-CAD. D. Confocal z-stack projections of E12.5 + 5 day wholemount immunostaining (n=3 *Stat3* cKO lungs). Green: SOX9; red: SOX2. Blue: Dapi. E. Sections of wild-type E12.5 lungs cultured for 3 days in 100nm Dx (left panel), or 100 nM Dx with 3 μM Mifepristone (right panel). Green: GR. GR staining is reduced in the presence lungs were cultured for 5 days in the presence of 3 μM Mifepristone, a Glucocorticoid inhibitor. G-I. Sections of *Stat3* cKO and sibling control lungs E12.5 + 5 days culture in Mifepristone. Two independent *Stat3* cKO lungs are shown (n=6 *Stat3* cKO lungs in two independent experiments). G. Green: E-CAD (epithelium); red: pSTAT3. H. Green: SOX9; red: SOX2; white: E-CAD. I. Green: pro-SFTPC; red: LAMP3. Bar = 50 μm B, C, E; 250 μm D; 100 μm G-I.

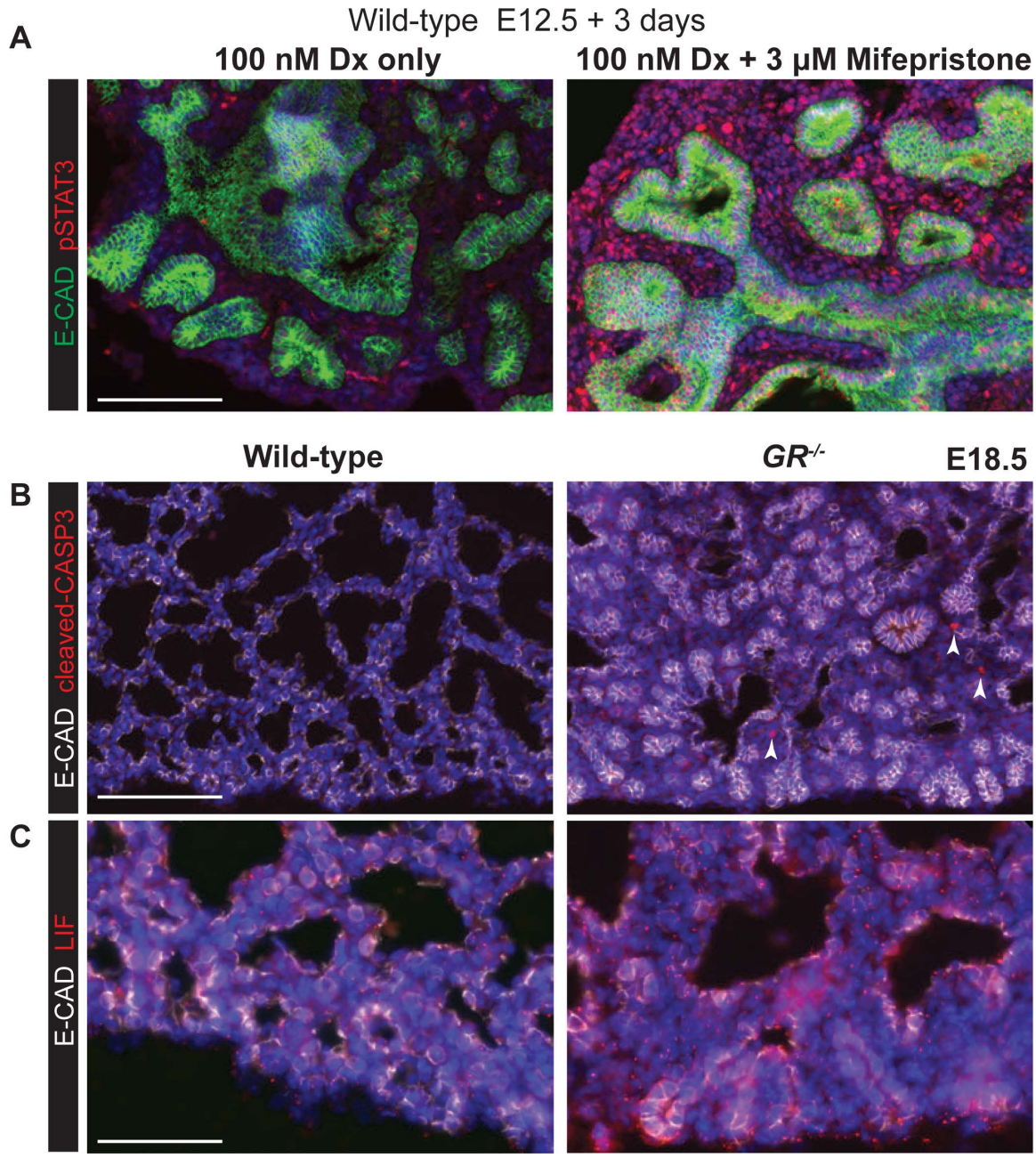


**Figure S8. STAT3 pathway activity in GR abrogated lungs.** A. Sections of wild-type E12.5 lungs cultured for 3 days in 100nm Dx (left panel), or 100 nM Dx with 3 µM Mifepristone (right panel). Green: E-CAD (epithelium); red: pSTAT3. B, C. Sections of *GR*$^{-/-}$ and sibling *GR*$^{+/+}$ control lungs. B. Red: cleaved-Caspase 3 (apoptotic cells); white: E-CAD (epithelium). Arrowheads mark a small number of apoptotic cells in the *GR*$^{-/-}$ lungs. C. Red: LIF; white: E-CAD (epithelium). Blue: Dapi. Bar = 100 µm A, B; 50 µm C.

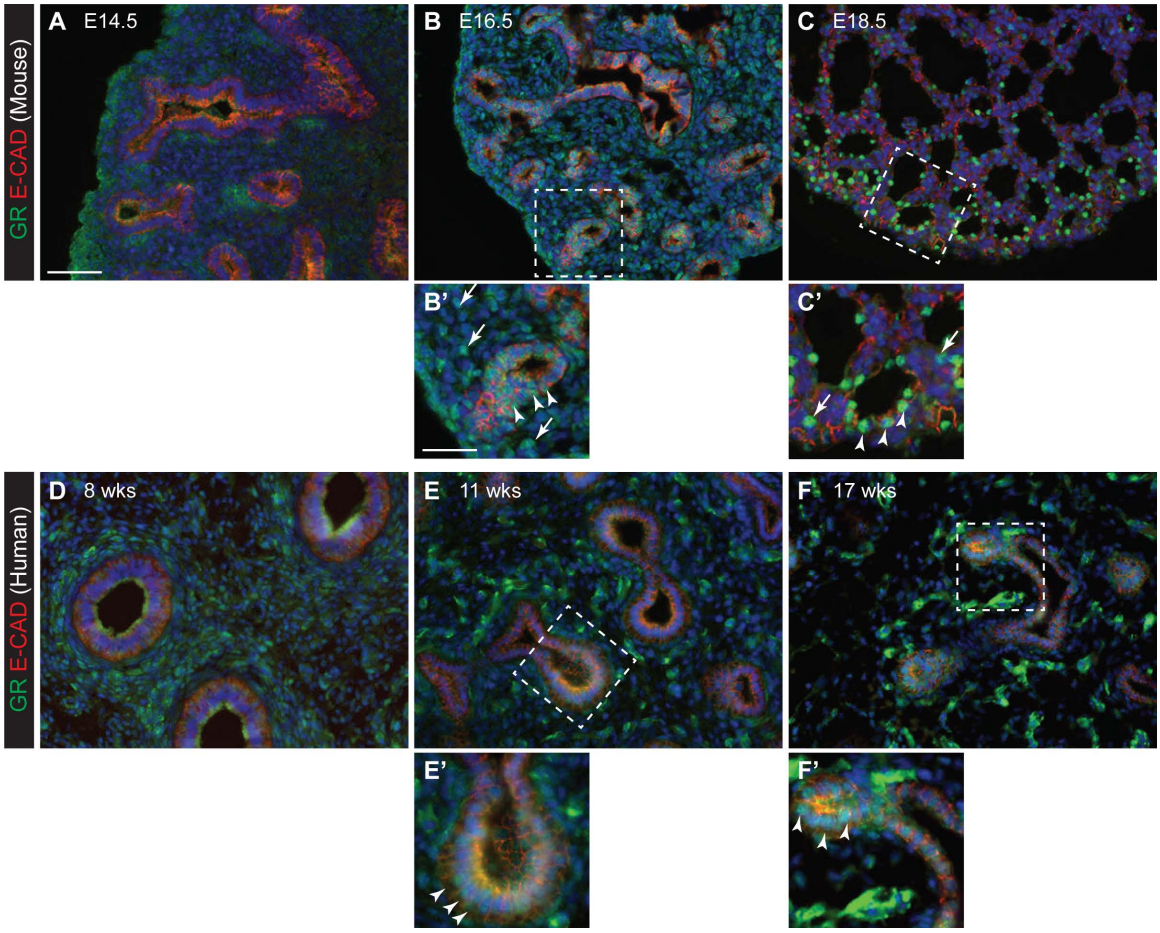


**Figure S9. GR staining in embryonic mouse and human lungs.** Sections of embryonic lungs stained for green: GR; red: E-CAD (epithelium); blue: Dapi. A-C. Mouse E14.5, 16.8 and 18.5. D-F. Human 8, 11 and 17 pcw. Boxed regions are blown up in B', C', E', F'. Arrow heads = $GR^+$ epithelial cells; arrows = $GR^+$ mesenchymal cells. Bar = 100 μm; 50 μm insets.

**Figure 4 - raw data table**

| Virus | Experiment number | Lung number | Total bronchiolar cells | GFP+ bronchiolar cells | Total alveolar cells | GFP+ alveolar cells | GFP+ bronchiolar cells / total bronchiolar cells (column E/ column D) | GFP+ alveolar cells / total alveolar cells (column G/column F) | Ratio GFP+ alveolar : bronchiolar (column I/column J) | Mean ratio GFP+ alveolar : bronchiolar | Standard deviation | 2-tailed T test versus GFP | Total E-CAD+ cells (column D + column F) | GFP+ E-CAD cells (column E + column G) | % GFP+ E-CAD cells (column P/column O *100) |
|---|---|---|---|---|---|---|---|---|---|---|---|---|---|---|---|
| **GFP** | ALC8 | 1 | 323 | 34 | 901 | 89 | 0.105263158 | 0.098779134 | 0.938401776 | | | | 1224 | 123 | 10.04901961 |
| | ALC8 | 2 | 161 | 14 | 665 | 81 | 0.086956522 | 0.121804511 | 1.40075188 | | | | 826 | 95 | 11.50121065 |
| | ALC10 | 3 | 478 | 29 | 953 | 79 | 0.060669456 | 0.082896118 | 1.366356696 | | | | 1431 | 108 | 7.547169811 |
| | ALC15 | 4 | 373 | 108 | 542 | 144 | 0.289544236 | 0.265682657 | 0.917589176 | | | | 915 | 252 | 27.54098361 |
| | ALC15 | 5 | 189 | 31 | 783 | 131 | 0.164021164 | 0.167305236 | 1.020022247 | | | | 972 | 162 | 16.66666667 |
| | ALC15 | 6 | 258 | 62 | 595 | 118 | 0.240310078 | 0.198319328 | 0.825264299 | 1.078064346 | 0.244857 | | 853 | 180 | 21.10199297 |
| **NOTCH** | ALC8 | 1 | 240 | 14 | 594 | 40 | 0.058333333 | 0.067340067 | 1.154401154 | | | | 834 | 54 | 6.474820144 |
| | ALC10 | 2 | 482 | 24 | 404 | 22 | 0.049792531 | 0.054455446 | 1.093646865 | | | | 886 | 46 | 5.191873589 |
| | ALC16 | 3 | 192 | 21 | 582 | 174 | 0.109375 | 0.298969072 | 2.733431517 | | | | 774 | 195 | 25.19379845 |
| | ALC16 | 4 | 274 | 44 | 239 | 76 | 0.160583942 | 0.317991632 | 1.980220616 | | | | 513 | 120 | 23.39181287 |
| | ALC16 | 5 | 377 | 64 | 578 | 74 | 0.169761273 | 0.128027682 | 0.754163062 | | | | 955 | 138 | 14.45026178 |
| | ALC16 | 6 | 279 | 38 | 1121 | 169 | 0.136200717 | 0.150758252 | 1.106882952 | | | | 1400 | 207 | 14.78571429 |
| | ALC16 | 7 | 596 | 88 | 301 | 34 | 0.147651007 | 0.112956811 | 0.765025672 | 1.369681691 | 0.72671 | 0.370618892 | 897 | 122 | 13.60089186 |
| **CEBPA** | ALC19 | 1 | 133 | 35 | 587 | 97 | 0.263157895 | 0.165247019 | 0.627938671 | | | | 720 | 132 | 18.33333333 |
| | ALC19 | 2 | 211 | 83 | 333 | 167 | 0.393364929 | 0.501501502 | 1.274901407 | | | | 544 | 250 | 45.95588235 |
| | ALC19 | 3 | 231 | 52 | 713 | 187 | 0.225108225 | 0.26227209 | 1.165093322 | | | | 944 | 239 | 25.31779661 |
| | ALC19 | 4 | 368 | 105 | 524 | 227 | 0.285326087 | 0.433206107 | 1.51828426 | | | | 892 | 332 | 37.21973094 |
| | ALC21 | 5 | 305 | 46 | 373 | 84 | 0.150819672 | 0.225201072 | 1.493181023 | | | | 678 | 130 | 19.1740413 |
| | ALC21 | 6 | 299 | 40 | 380 | 63 | 0.133779264 | 0.165789474 | 1.239276316 | | | | 679 | 103 | 15.16936672 |
| | ALC21 | 7 | 322 | 47 | 289 | 64 | 0.145962733 | 0.221453287 | 1.517190606 | | | | 611 | 111 | 18.16693944 |
| | ALC21 | 8 | 398 | 58 | 441 | 87 | 0.145728643 | 0.197278912 | 1.353741497 | 1.273700888 | 0.293666 | 0.211391815 | 839 | 145 | 17.28247914 |
| **CITED2** | ALC8 | 1 | 176 | 4 | 304 | 12 | 0.022727273 | 0.039473684 | 1.736842105 | | | | 480 | 16 | 3.333333333 |
| | ALC8 | 2 | 465 | 18 | 970 | 105 | 0.038709677 | 0.108247423 | 2.796391753 | | | | 1435 | 123 | 8.571428571 |
| | ALC17 | 3 | 58 | 5 | 1007 | 156 | 0.086206897 | 0.154915591 | 1.797020854 | | | | 1065 | 161 | 15.11737089 |
| | ALC17 | 4 | 685 | 50 | 553 | 97 | 0.072992701 | 0.175406872 | 2.403074141 | | | | 1238 | 147 | 11.87399031 |
| | ALC17 | 5 | 191 | 46 | 560 | 206 | 0.240837696 | 0.367857143 | 1.527406832 | 2.052147137 | 0.52842 | 0.002865192 | 751 | 252 | 33.55525965 |
| **STAT3.1** | ALC14 | 1 | 390 | 72 | 1220 | 403 | 0.184615385 | 0.330327869 | 1.789275956 | | | | 1610 | 475 | 29.50310559 |
| | ALC14 | 2 | 452 | 89 | 628 | 94 | 0.196902655 | 0.149681529 | 0.760180348 | | | | 1080 | 183 | 16.94444444 |
| | ALC20 | 3 | 283 | 25 | 477 | 118 | 0.088339223 | 0.247379455 | 2.80033543 | | | | 760 | 143 | 18.81578947 |
| | ALC20 | 4 | 148 | 14 | 254 | 86 | 0.094594595 | 0.338582677 | 3.579302587 | | | | 402 | 100 | 24.87562189 |
| | ALC20 | 5 | 85 | 15 | 396 | 107 | 0.176470588 | 0.27020202 | 1.531144781 | | | | 481 | 122 | 25.36382536 |
| | ALC20 | 6 | 61 | 11 | 322 | 110 | 0.180327869 | 0.341614907 | 1.894409938 | | | | 383 | 121 | 31.5926893 |
| | ALC22 | 7 | 283 | 25 | 477 | 118 | 0.088339223 | 0.247379455 | 2.80033543 | | | | 760 | 143 | 18.81578947 |
| | ALC22 | 8 | 148 | 14 | 254 | 86 | 0.094594595 | 0.338582677 | 3.579302587 | 2.341785882 | 1.010478 | 0.01169454 | 402 | 100 | 24.87562189 |
| **STAT3.2** | ALC20 | 1 | 219 | 26 | 466 | 107 | 0.118721461 | 0.229613734 | 1.934054143 | | | | 685 | 133 | 19.41605839 |
| | ALC20 | 2 | 259 | 15 | 292 | 44 | 0.057915058 | 0.150684932 | 2.601826484 | | | | 551 | 59 | 10.70780399 |
| | ALC22 | 3 | 318 | 24 | 475 | 86 | 0.075471698 | 0.181052632 | 2.398947368 | | | | 793 | 110 | 13.87137453 |
| | ALC22 | 4 | 812 | 54 | 335 | 45 | 0.066502463 | 0.134328358 | 2.019900498 | | | | 1147 | 99 | 8.631211857 |
| | ALC22 | 5 | 420 | 36 | 474 | 82 | 0.085714286 | 0.172995781 | 2.018284107 | 2.19460252 | 0.290294 | 0.000142186 | 894 | 118 | 13.19910515 |
| **STAT5A.1** | ALC12 | 1 | 409 | 7 | 739 | 43 | 0.017114914 | 0.058186739 | 3.399768026 | | | | 1148 | 50 | 4.355400697 |
| | ALC12 | 2 | 100 | 1 | 539 | 19 | 0.01 | 0.035250464 | 3.525046382 | | | | 639 | 20 | 3.129890454 |
| | ALC12 | 3 | 302 | 9 | 971 | 43 | 0.029801325 | 0.044284243 | 1.485982378 | | | | 1273 | 52 | 4.084838963 |
| | ALC17 | 4 | 664 | 88 | 912 | 270 | 0.13253012 | 0.296052632 | 2.233851675 | | | | 1576 | 358 | 22.71573604 |
| | ALC17 | 5 | 367 | 53 | 1034 | 244 | 0.144414169 | 0.235976789 | 1.634027955 | | | | 1401 | 297 | 21.19914347 |
| | ALC17 | 6 | 190 | 12 | 557 | 76 | 0.063157895 | 0.136445242 | 2.160383004 | 2.406509903 | 0.868582 | 0.004801348 | 747 | 88 | 11.78045515 |
| **STAT5A.2** | ALC12 | 1 | 570 | 23 | 808 | 71 | 0.040350877 | 0.087871287 | 2.177679724 | | | | 1378 | 94 | 6.821480406 |
| | ALC12 | 2 | 388 | 15 | 489 | 64 | 0.038659794 | 0.130879346 | 3.385412406 | | | | 877 | 79 | 9.007981756 |
| | ALC18 | 3 | 615 | 89 | 942 | 261 | 0.144715447 | 0.277070064 | 1.914585272 | | | | 1557 | 350 | 22.47912653 |
| | ALC18 | 4 | 617 | 98 | 561 | 223 | 0.158833063 | 0.397504456 | 2.502655608 | 2.495083253 | 0.640434 | 0.001027725 | 1178 | 321 | 27.24957555 |
| **STAT6** | ALC19 | 1 | 97 | 12 | 476 | 105 | 0.12371134 | 0.220588235 | 1.783088235 | | | | 573 | 117 | 20.41884817 |
| | ALC19 | 2 | 182 | 47 | 345 | 103 | 0.258241758 | 0.298550725 | 1.15609004 | | | | 527 | 150 | 28.4629981 |
| | ALC19 | 3 | 452 | 56 | 542 | 115 | 0.123893805 | 0.212177122 | 1.712572483 | | | | 994 | 171 | 17.20321932 |
| | ALC19 | 4 | 313 | 20 | 416 | 64 | 0.063897764 | 0.153846154 | 2.407692308 | 1.764860766 | 0.512152 | 0.020296067 | 729 | 84 | 11.52263374 |

## SUPPLEMENTAL FIGURES

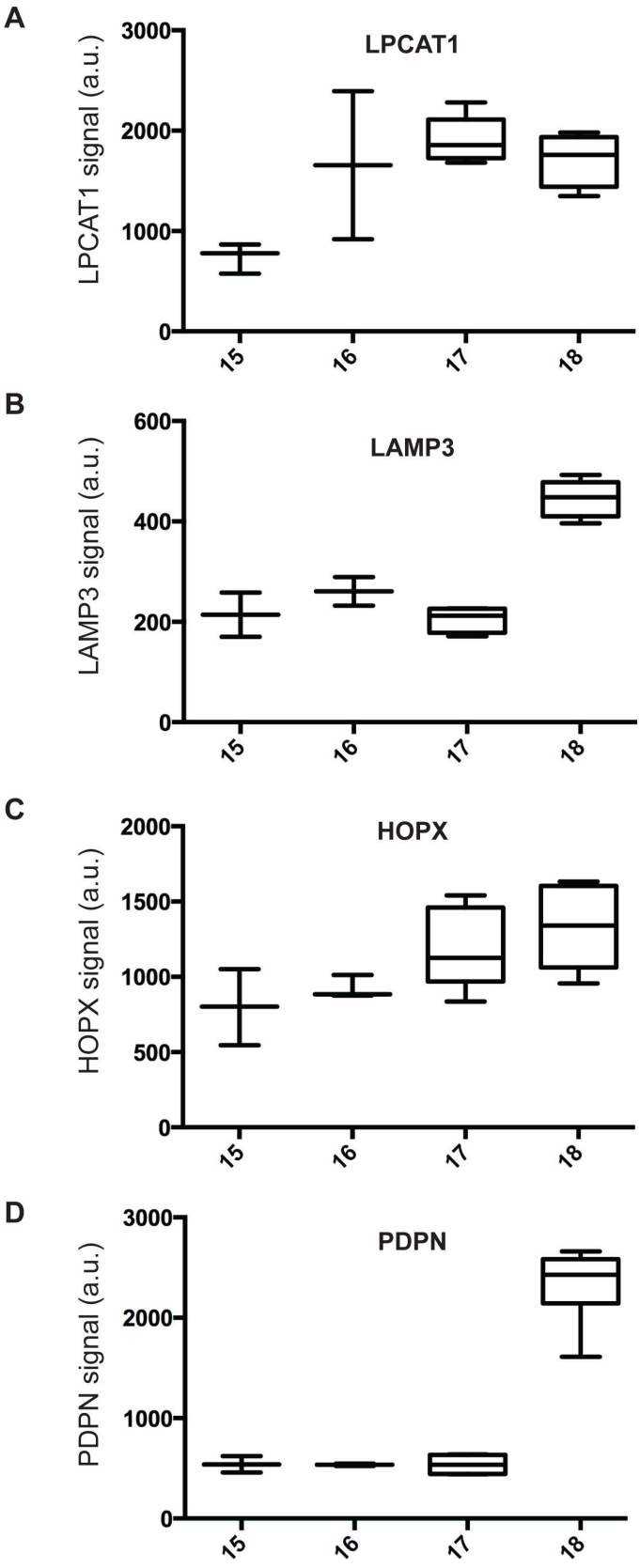

**Figure S1. Relative expression level of alveolar epithelial fate markers in normal lung development over time.** Bar and whisker plots showing relative expression levels of alveolar fate markers analysed in Figure 1 in arbitrary units normalized to the total cell area sampled. A. LPCAT1 (raw data from images underpinning Fig. 1D). B. LAMP3 (raw data from images underpinning Fig 1D). C. HOPX (raw data from images underpinning Fig. 1F). D. PDPN (raw data from images underpinning Fig. 1D).

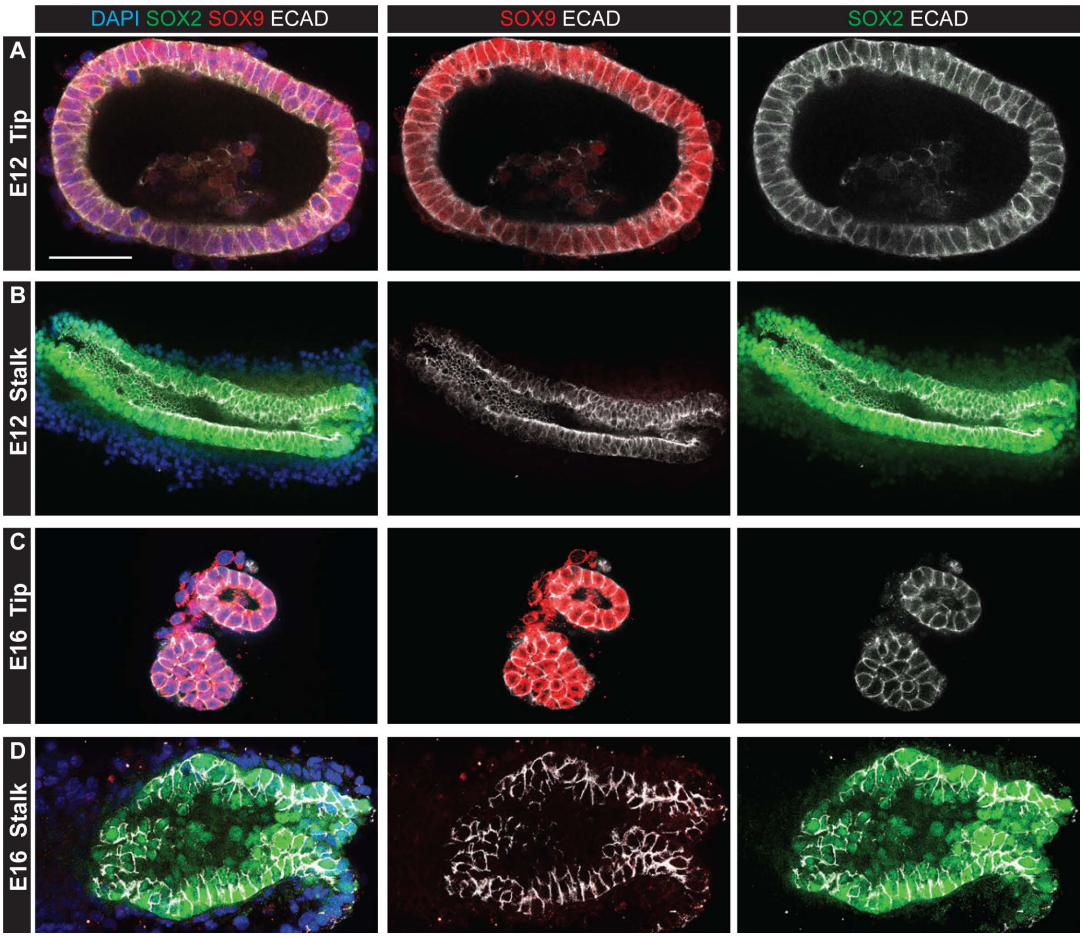


**Figure S2. Microdissected tip and stalk cells.** Examples of wholemount stained microdissected tip and stalk cells. Green: SOX2 (stalk/differentiating bronchioles); red: SOX9 (tip); white: E-CAD (epithelium); blue: DAPI (nuclei). A. E12.5 tip. B. E12.5 stalk. C. E16.5 tip. D. E16.5 stalk. Bars = 50 μm A,C,D; 100 μm B.

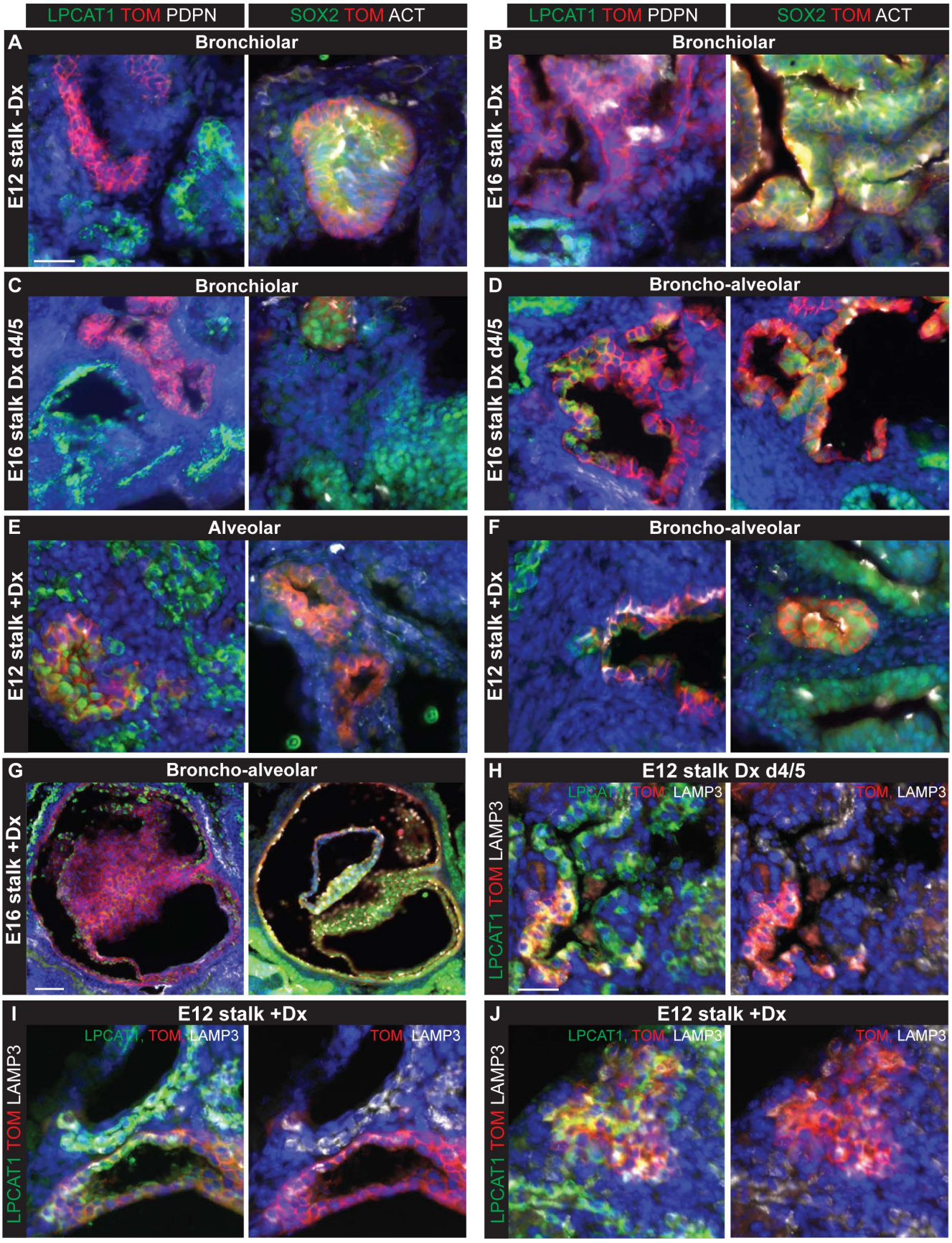

**Figure S3. Grafted stalk cells can respond to the host environment and alter progeny cell fate.** Examples of grafted stalk cells following 8 days of culture in various conditions. A-G. Two images of each graft are shown taken from adjacent slides stained to detect alveolar fate: green: LPCAT1 (alveolar fate); red: Tomato fluorescence (grafted cells); white: PDPN (basal and type 1 cells), or bronchiolar fate: green: SOX2 (bronchiolar fate); red: RFP (Tomato$^{+}$ graft); white: acetylated tubulin (cilia) to determine graft fate. A. E12.5 stalk, no Dx, bronchiolar-fated. B. E16.5 stalk, no Dx, bronchiolar-fated. C. E16.5 stalk, Dx day4/5, bronchiolar fated. D. E16.5 stalk, Dx day4/5, mixed broncho-alveolar fated. E. E12.5 stalk, Dx throughout, alveolar fated. F. E12.5 stalk, Dx throughout, mixed broncho-alveolar fated. G. E16.5 stalk, Dx throughout, mixed broncho-alveolar fated. H-J. Grafts are stained to detect alveolar markers. Green: LPCAT1 (alveolar fate); red: Tomato fluorescence (grafted cells); white: LAMP3 (differentiating AT2 cells). Right panel has the green channel removed to show the Tomato/LAMP3 co-localisation clearly. H. E12.5 stalk, Dx day4/5. I, J. E12.5 stalk, Dx throughout. Bars = 50 μm C left panel; 100 μm all other panels.

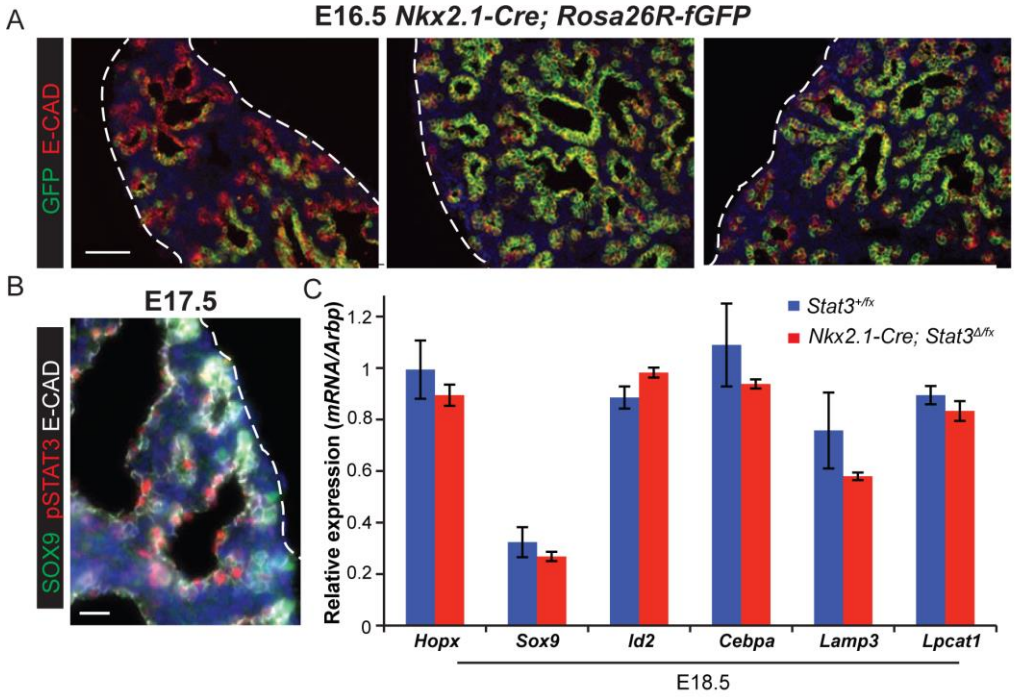


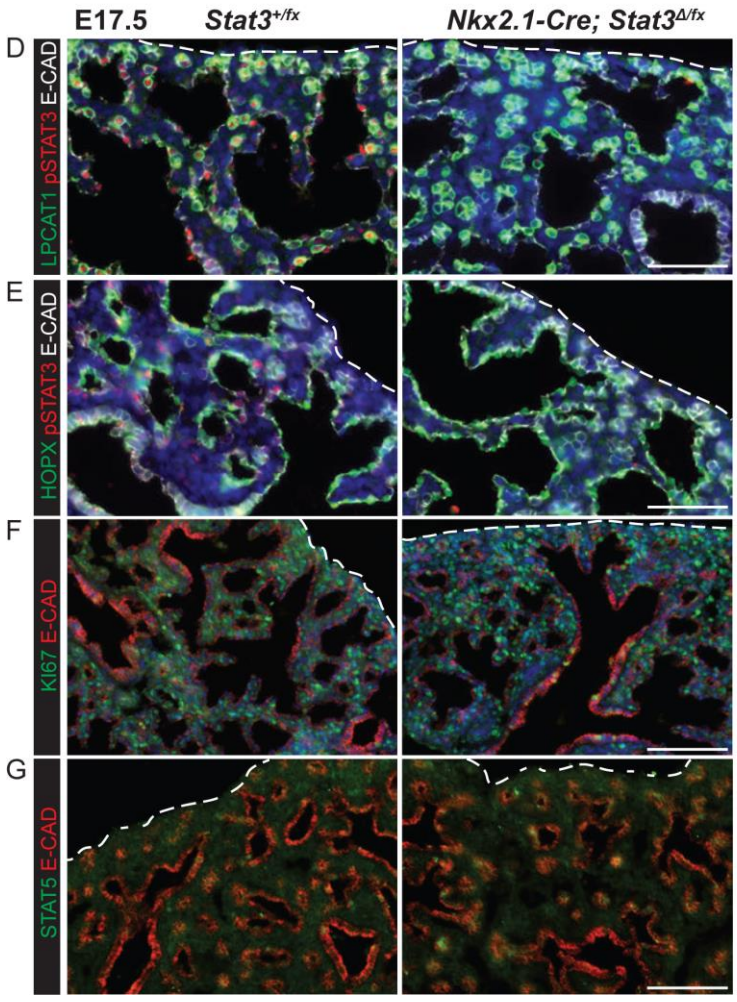


H

**% alveolar epithelial cells expressing LPCAT1**

| | *Stat3*$^{+/fx}$ | *Nkx2.1-Cre; Stat3*$^{\Delta/fx}$ |
|---|---|---|
| E17.5 | 79 +/- 2.3% | 81 +/- 2.2% |
| E18.5 | 70 +/- 0.5% | 71 +/- 2.6% |

**% alveolar epithelial cells expressing HOPX**

| | *Stat3*$^{+/fx}$ | *Nkx2.1-Cre; Stat3*$^{\Delta/fx}$ |
|---|---|---|
| E17.5 | 69 +/- 1.3% | 67 +/- 2% |
| E18.5 | 52 +/- 1.1% | 57 +/- 2.1% |

**Figure S4. Alveolar maturation ultimately occurs in the *Stat3* cKO lungs.** A. Sections of E16.5 *Nkx2.1-Cre; Rosa26R-fGFP* lungs illustrating variation in the extent of recombination. Green: eGFP (reporter); red: E-CAD (epithelium). B. Section of E17.5 wild-type lung illustrating that pSTAT3 is predominantly seen in differentiating cells that have exited the tip. Green: SOX9 (tip); red: pSTAT3; white: E-CAD (epithelium). C. RT-qPCR of progenitor and alveolar markers from *Nkx2.1-Cre; Stat3*$^{\Delta/fx}$ and sibling *Stat3*$^{fx/+}$ control E18.5 lungs. Error bars = s.e.m. D, E. Sections of *Stat3* cKO and sibling lungs. D. Green: LPCAT1 (late tip and AT2 cells); red: pSTAT3; white: E-CAD (epithelium). E. Green: HOPX (differentiating AT1 cells); red: pSTAT3; white: E-CAD (epithelium). F: Green: Ki67 (proliferating cells); red: E-CAD (epithelium); blue: Dapi. G. Green: STAT5; red: E-CAD (epithelium). H. Quantification of LPCAT1 and HOPX staining in E17.5 and E18.5 *Nkx2.1-Cre; Stat3*$^{\Delta/fx}$ and sibling *Stat3*$^{fx/+}$ control. Mean and s.e.m. are displayed for 3 independent samples. Bar = 50 µm A, D, E; 25 µm B; 100 µm F, G.

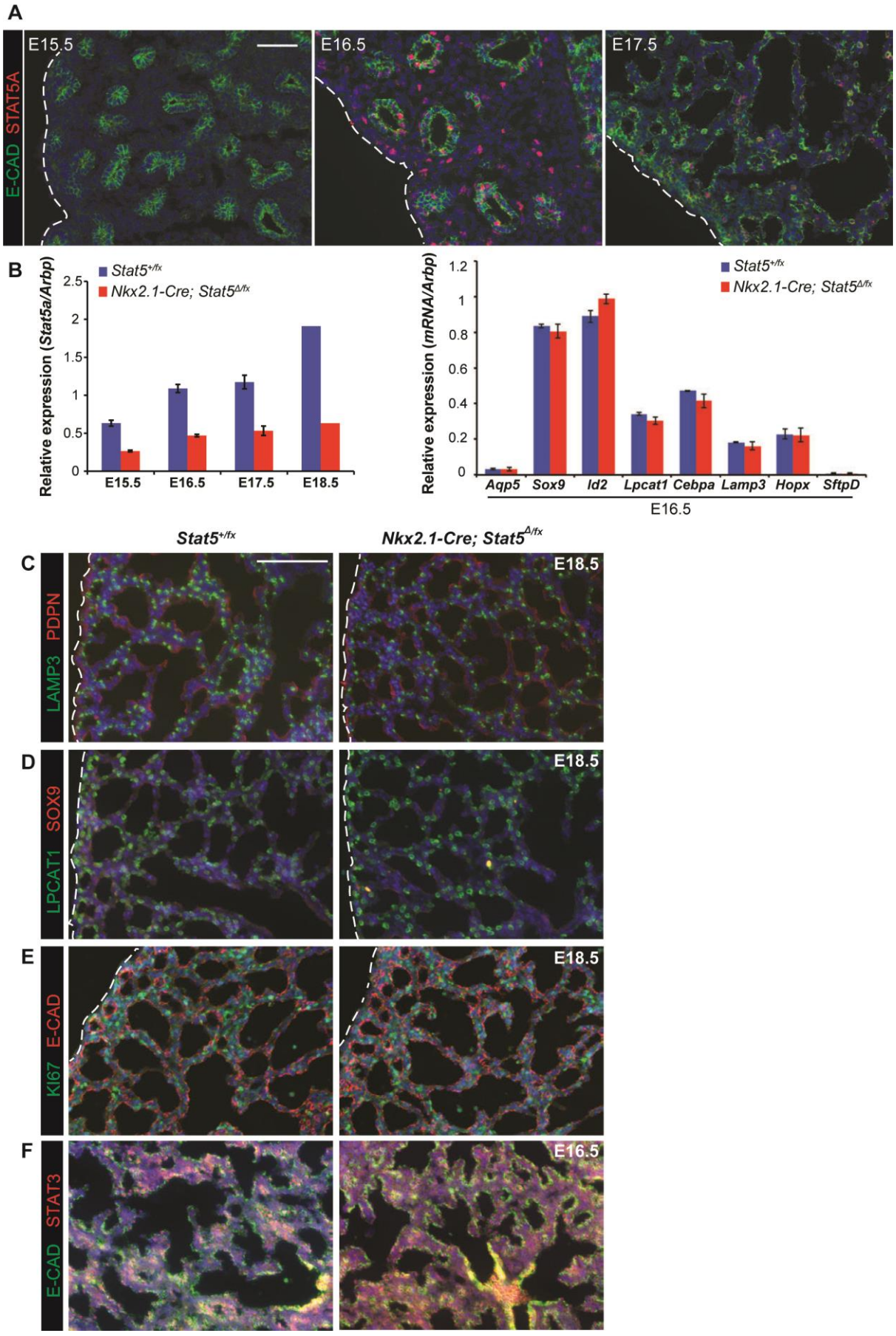

**Figure S5. Lung epithelial specific knock-out of *Stat5a/b* does not result in alveolar differentiation phenotypes.** A. Wild-type E15.5, 16.5, 17.5 lung sections. Green: E-CAD (epithelium); Red: STAT5A. B. RT-qPCR of *Stat5a* and progenitor/alveolar markers from *Nkx2.1-Cre; Stat5*$^{\Delta/fx}$ and sibling *Stat5*$^{fx/+}$ control lungs. Error bars = s.e.m. C-F. Sections of *Stat5* cKO and sibling control lungs. C. E18.5. Green: LAMP3 (differentiating AT2 cells); red: PDPN (AT1 cells). D. E18.5. Green: LPCAT1 (AT2 cells); red: SOX9 (progenitor cells). E. E18.5. Green: KI67 (proliferating cells); red: E-CAD (epithelium). F. E16.5. Green: E-CAD (epithelium); red: STAT3. At each time-point, three independent litters were collected and stained. Blue: Dapi. Bar = 50 μm A, E, F; 100 μm C,D.

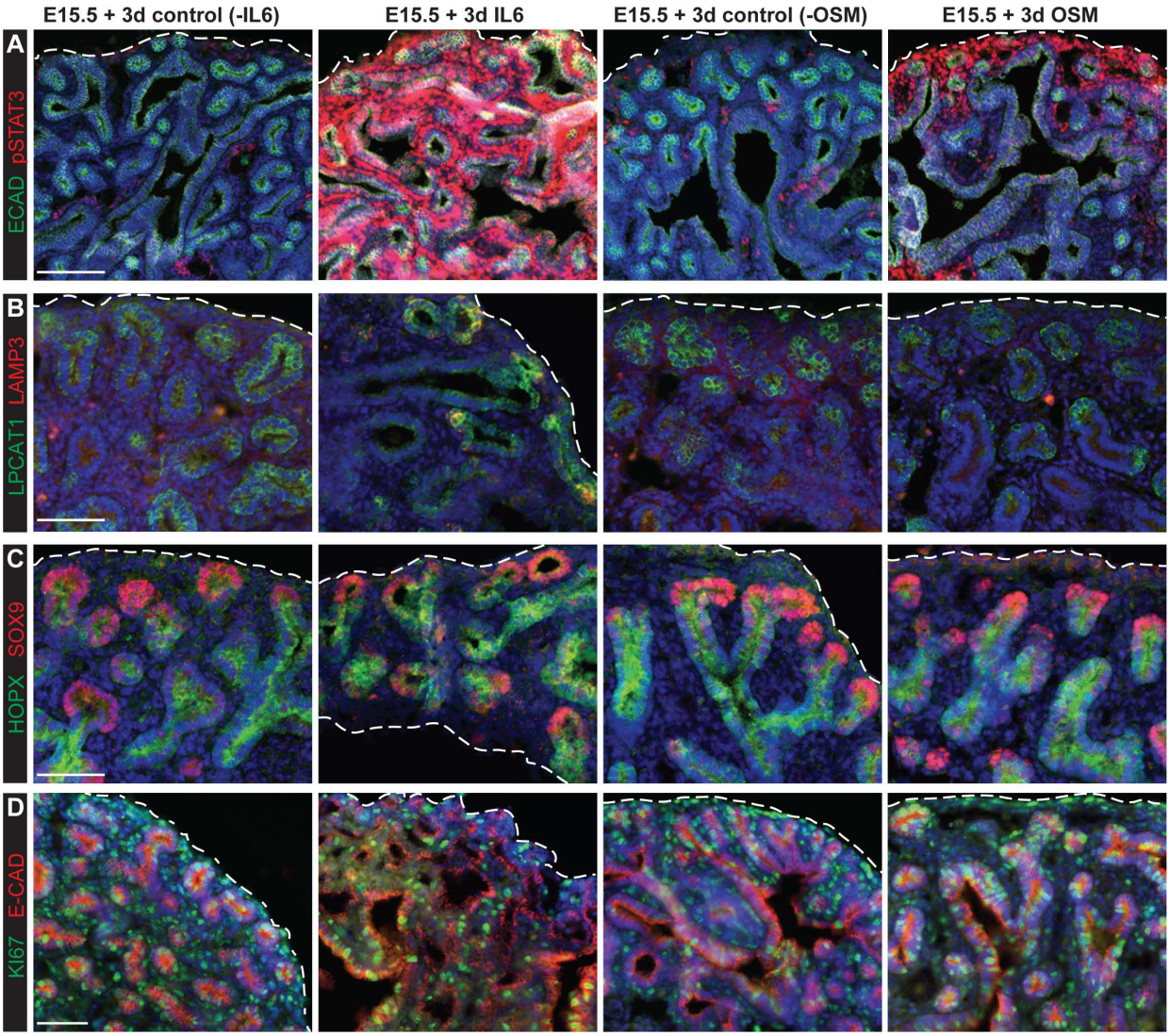


**Figure S6. Activating pSTAT3 via OSM is not sufficient to accelerate AT2 differentiation.** Sections of E15.5 lung slices cultured for 3 days +/- 10 ng/ml IL6, or +/- 25 ng/ml OSM. A. Green: E-CAD (epithelium); red (pSTAT3). B. Green: LPCAT1 (late tip and AT2); red: LAMP3 (AT2). C. Green: HOPX (stalk cells from E16.5, AT1 cells); red: SOX9. D. Green: KI67 (proliferating cells); red: E-CAD (epithelium); Blue: Dapi. Bar = 100 μm A; 50 μm B-D.

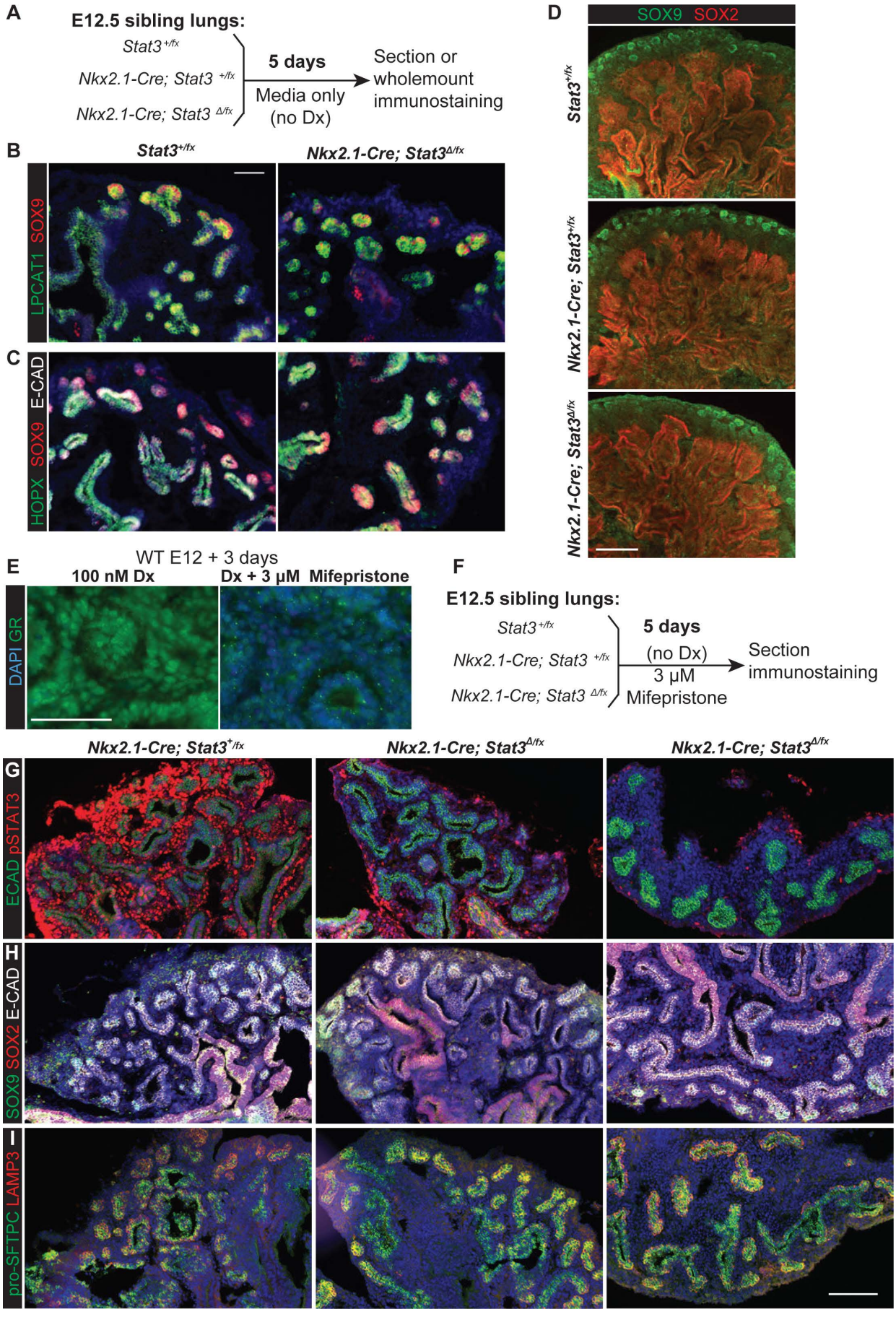

**Figure S7. No evidence for redundant Glucocorticoid and STAT3 activity in alveolar development.** A. Experimental scheme: E12.5 *Stat3* cKO and sibling control lungs were cultured for 5 days in the absence of exogenous glucocorticoid. B, C. E12.5 + 5 day sections (n=6 *Stat3* cKO lungs in two independent experiments). B. Green: LPCAT1; red: SOX9. C. Green: HOPX; red: SOX9; white: E-CAD. D. Confocal z-stack projections of E12.5 + 5 day wholemount immunostaining (n=3 *Stat3* cKO lungs). Green: SOX9; red: SOX2. Blue: Dapi. E. Sections of wild-type E12.5 lungs cultured for 3 days in 100nm Dx (left panel), or 100 nM Dx with 3 μM Mifepristone (right panel). Green: GR. GR staining is reduced in the presence lungs were cultured for 5 days in the presence of 3 μM Mifepristone, a Glucocorticoid inhibitor. G-I. Sections of *Stat3* cKO and sibling control lungs E12.5 + 5 days culture in Mifepristone. Two independent *Stat3* cKO lungs are shown (n=6 *Stat3* cKO lungs in two independent experiments). G. Green: E-CAD (epithelium); red: pSTAT3. H. Green: SOX9; red: SOX2; white: E-CAD. I. Green: pro-SFTPC; red: LAMP3. Bar = 50 μm B, C, E; 250 μm D; 100 μm G-I.

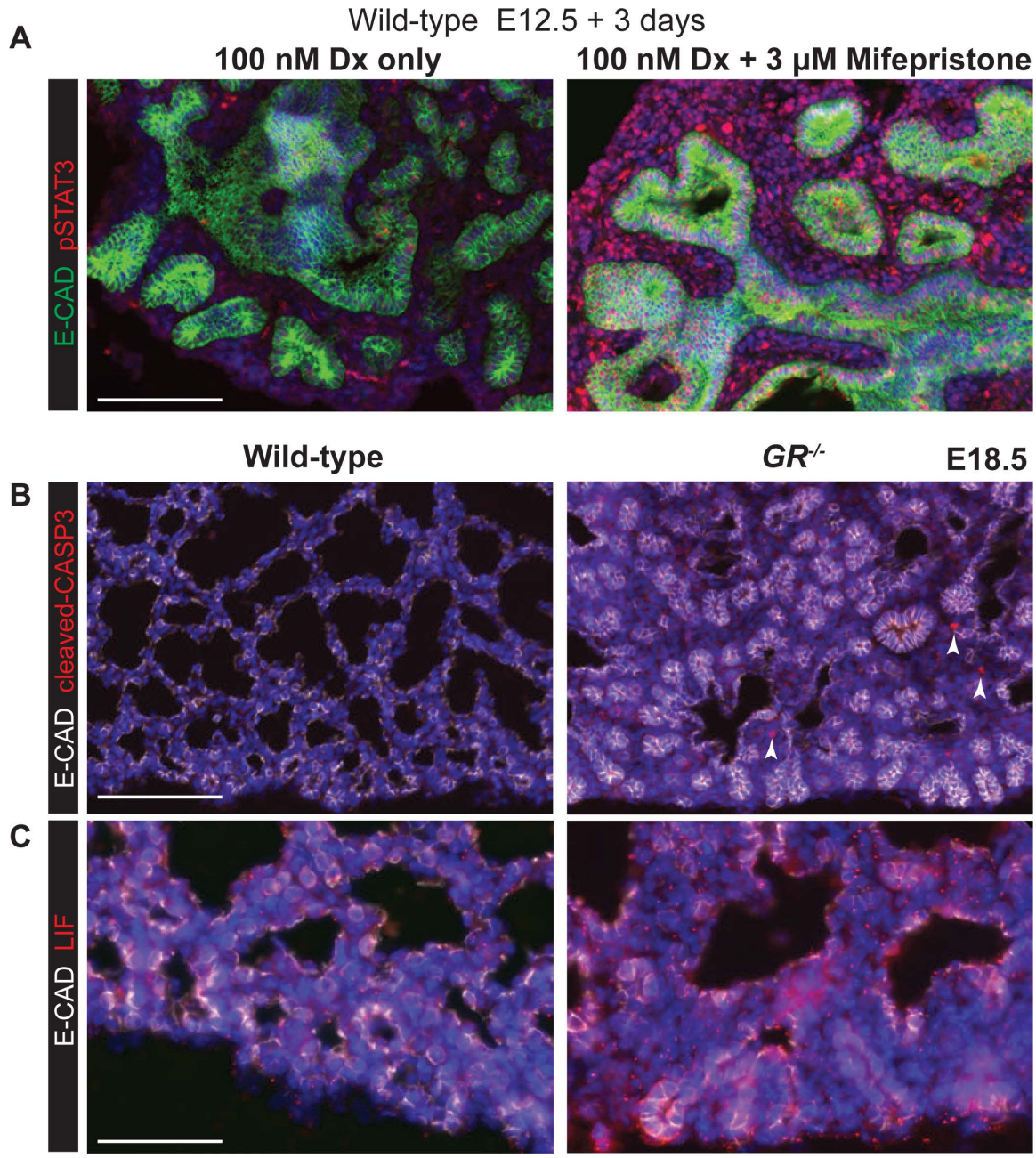


**Figure S8. STAT3 pathway activity in GR abrogated lungs.** A. Sections of wild-type E12.5 lungs cultured for 3 days in 100nm Dx (left panel), or 100 nM Dx with 3 µM Mifepristone (right panel). Green: E-CAD (epithelium); red: pSTAT3. B, C. Sections of *GR*$^{-/-}$ and sibling *GR*$^{+/+}$ control lungs. B. Red: cleaved-Caspase 3 (apoptotic cells); white: E-CAD (epithelium). Arrowheads mark a small number of apoptotic cells in the *GR*$^{-/-}$ lungs. C. Red: LIF; white: E-CAD (epithelium). Blue: Dapi. Bar = 100 µm A, B; 50 µm C.

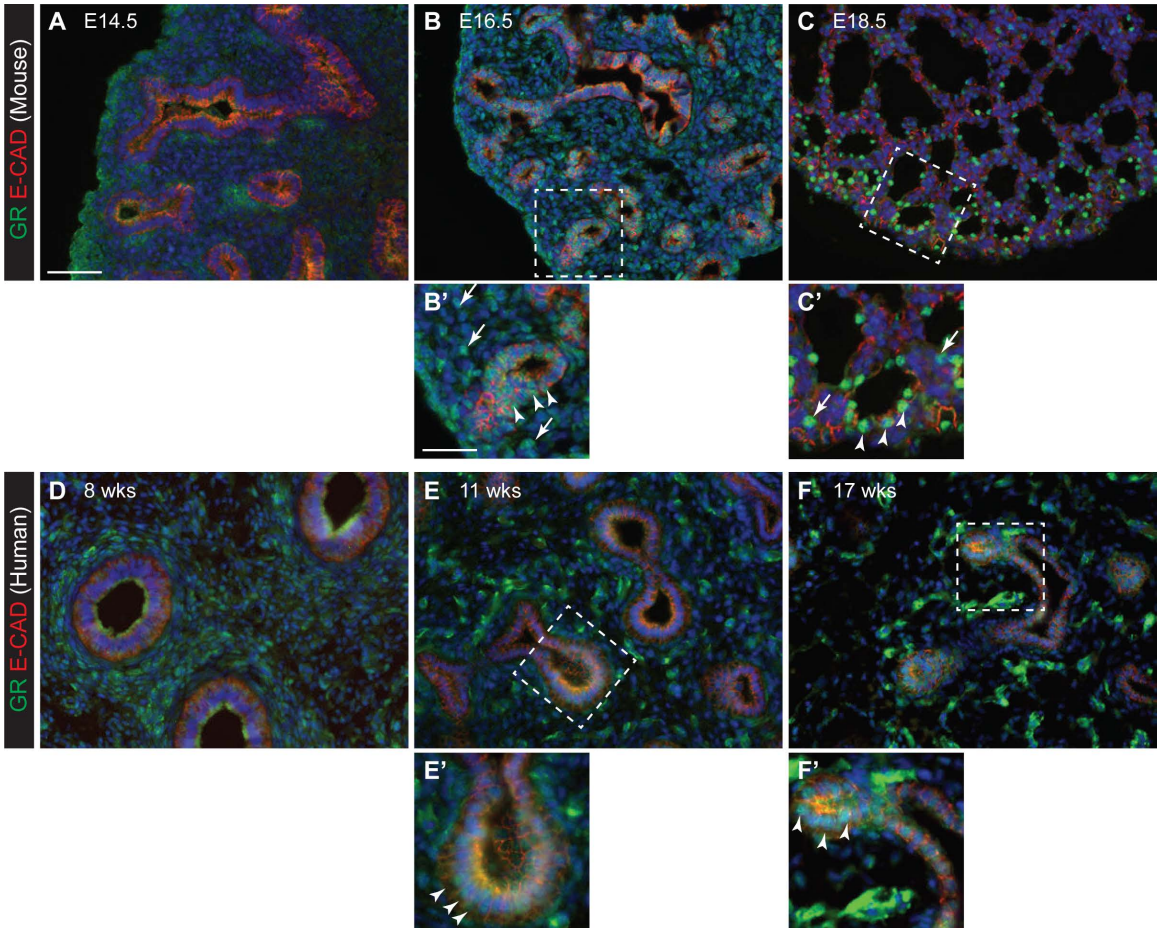


**Figure S9. GR staining in embryonic mouse and human lungs.** Sections of embryonic lungs stained for green: GR; red: E-CAD (epithelium); blue: Dapi. A-C. Mouse E14.5, 16.8 and 18.5. D-F. Human 8, 11 and 17 pcw. Boxed regions are blown up in B', C', E', F'. Arrow heads = $GR^+$ epithelial cells; arrows = $GR^+$ mesenchymal cells. Bar = 100 μm; 50 μm insets.

# Table S1. Raw data accompanying Fig. 4.

| Virus | Experiment number | Lung number | Total bronchiolar cells | GFP+ bronchiolar cells | Total alveolar cells | GFP+ alveolar cells | GFP+ bronchiolar cells / total bronchiolar cells (column E/ column D) | GFP+ alveolar cells / total alveolar cells (column G/column F) | Ratio GFP+ alveolar : bronchiolar (column I/column J) | Mean ratio GFP+ alveolar : bronchiolar | Standard deviation | 2-tailed T test versus GFP | Total E-CAD+ cells (column D + column F) | GFP+ E-CAD cells (column E + column G) | % GFP+ E-CAD cells (column P/column O *100) |
|---|---|---|---|---|---|---|---|---|---|---|---|---|---|---|---|
| **GFP** | ALC8 | 1 | 323 | 34 | 901 | 89 | 0.105263158 | 0.098779134 | 0.938401776 | | | | 1224 | 123 | 10.04901961 |
| | ALC8 | 2 | 161 | 14 | 665 | 81 | 0.086956522 | 0.121804511 | 1.40075188 | | | | 826 | 95 | 11.50121065 |
| | ALC10 | 3 | 478 | 29 | 953 | 79 | 0.060669456 | 0.082896118 | 1.366356696 | | | | 1431 | 108 | 7.547169811 |
| | ALC15 | 4 | 373 | 108 | 542 | 144 | 0.289544236 | 0.265682657 | 0.917589176 | | | | 915 | 252 | 27.54098361 |
| | ALC15 | 5 | 189 | 31 | 783 | 131 | 0.164021164 | 0.167305236 | 1.020022247 | | | | 972 | 162 | 16.66666667 |
| | ALC15 | 6 | 258 | 62 | 595 | 118 | 0.240310078 | 0.198319328 | 0.825264299 | 1.078064346 | 0.244857 | | 853 | 180 | 21.10199297 |
| **NOTCH** | ALC8 | 1 | 240 | 14 | 594 | 40 | 0.058333333 | 0.067340067 | 1.154401154 | | | | 834 | 54 | 6.474820144 |
| | ALC10 | 2 | 482 | 24 | 404 | 22 | 0.049792531 | 0.054455446 | 1.093646865 | | | | 886 | 46 | 5.191873589 |
| | ALC16 | 3 | 192 | 21 | 582 | 174 | 0.109375 | 0.298969072 | 2.733431517 | | | | 774 | 195 | 25.19379845 |
| | ALC16 | 4 | 274 | 44 | 239 | 76 | 0.160583942 | 0.317991632 | 1.980220616 | | | | 513 | 120 | 23.39181287 |
| | ALC16 | 5 | 377 | 64 | 578 | 74 | 0.169761273 | 0.128027682 | 0.754163062 | | | | 955 | 138 | 14.45026178 |
| | ALC16 | 6 | 279 | 38 | 1121 | 169 | 0.136200717 | 0.150758252 | 1.106882952 | | | | 1400 | 207 | 14.78571429 |
| | ALC16 | 7 | 596 | 88 | 301 | 34 | 0.147651007 | 0.112956811 | 0.765025672 | 1.369681691 | 0.72671 | 0.370618892 | 897 | 122 | 13.60089186 |
| **CEBPA** | ALC19 | 1 | 133 | 35 | 587 | 97 | 0.263157895 | 0.165247019 | 0.627938671 | | | | 720 | 132 | 18.33333333 |
| | ALC19 | 2 | 211 | 83 | 333 | 167 | 0.393364929 | 0.501501502 | 1.274901407 | | | | 544 | 250 | 45.95588235 |
| | ALC19 | 3 | 231 | 52 | 713 | 187 | 0.225108225 | 0.26227209 | 1.165093322 | | | | 944 | 239 | 25.31779661 |
| | ALC19 | 4 | 368 | 105 | 524 | 227 | 0.285326087 | 0.433206107 | 1.51828426 | | | | 892 | 332 | 37.21973094 |
| | ALC21 | 5 | 305 | 46 | 373 | 84 | 0.150819672 | 0.225201072 | 1.493181023 | | | | 678 | 130 | 19.1740413 |
| | ALC21 | 6 | 299 | 40 | 380 | 63 | 0.133779264 | 0.165789474 | 1.239276316 | | | | 679 | 103 | 15.16936672 |
| | ALC21 | 7 | 322 | 47 | 289 | 64 | 0.145962733 | 0.221453287 | 1.517190606 | | | | 611 | 111 | 18.16693944 |
| | ALC21 | 8 | 398 | 58 | 441 | 87 | 0.145728643 | 0.197278912 | 1.353741497 | 1.273700888 | 0.293666 | 0.211391815 | 839 | 145 | 17.28247914 |
| **CITED2** | ALC8 | 1 | 176 | 4 | 304 | 12 | 0.022727273 | 0.039473684 | 1.736842105 | | | | 480 | 16 | 3.333333333 |
| | ALC8 | 2 | 465 | 18 | 970 | 105 | 0.038709677 | 0.108247423 | 2.796391753 | | | | 1435 | 123 | 8.571428571 |
| | ALC17 | 3 | 58 | 5 | 1007 | 156 | 0.086206897 | 0.154915591 | 1.797020854 | | | | 1065 | 161 | 15.11737089 |
| | ALC17 | 4 | 685 | 50 | 553 | 97 | 0.072992701 | 0.175406872 | 2.403074141 | | | | 1238 | 147 | 11.87399031 |
| | ALC17 | 5 | 191 | 46 | 560 | 206 | 0.240837696 | 0.367857143 | 1.527406832 | 2.052147137 | 0.52842 | 0.002865192 | 751 | 252 | 33.55525965 |
| **STAT3.1** | ALC14 | 1 | 390 | 72 | 1220 | 403 | 0.184615385 | 0.330327869 | 1.789275956 | | | | 1610 | 475 | 29.50310559 |
| | ALC14 | 2 | 452 | 89 | 628 | 94 | 0.196902655 | 0.149681529 | 0.760180348 | | | | 1080 | 183 | 16.94444444 |
| | ALC20 | 3 | 283 | 25 | 477 | 118 | 0.088339223 | 0.247379455 | 2.80033543 | | | | 760 | 143 | 18.81578947 |
| | ALC20 | 4 | 148 | 14 | 254 | 86 | 0.094594595 | 0.338582677 | 3.579302587 | | | | 402 | 100 | 24.87562189 |
| | ALC20 | 5 | 85 | 15 | 396 | 107 | 0.176470588 | 0.27020202 | 1.531144781 | | | | 481 | 122 | 25.36382536 |
| | ALC20 | 6 | 61 | 11 | 322 | 110 | 0.180327869 | 0.341614907 | 1.894409938 | | | | 383 | 121 | 31.5926893 |
| | ALC22 | 7 | 283 | 25 | 477 | 118 | 0.088339223 | 0.247379455 | 2.80033543 | | | | 760 | 143 | 18.81578947 |
| | ALC22 | 8 | 148 | 14 | 254 | 86 | 0.094594595 | 0.338582677 | 3.579302587 | 2.341785882 | 1.010478 | 0.01169454 | 402 | 100 | 24.87562189 |
| **STAT3.2** | ALC20 | 1 | 219 | 26 | 466 | 107 | 0.118721461 | 0.229613734 | 1.934054143 | | | | 685 | 133 | 19.41605839 |
| | ALC20 | 2 | 259 | 15 | 292 | 44 | 0.057915058 | 0.150684932 | 2.601826484 | | | | 551 | 59 | 10.70780399 |
| | ALC22 | 3 | 318 | 24 | 475 | 86 | 0.075471698 | 0.181052632 | 2.398947368 | | | | 793 | 110 | 13.87137453 |
| | ALC22 | 4 | 812 | 54 | 335 | 45 | 0.066502463 | 0.134328358 | 2.019900498 | | | | 1147 | 99 | 8.631211857 |
| | ALC22 | 5 | 420 | 36 | 474 | 82 | 0.085714286 | 0.172995781 | 2.018284107 | 2.19460252 | 0.290294 | 0.000142186 | 894 | 118 | 13.19910515 |
| **STAT5A.1** | ALC12 | 1 | 409 | 7 | 739 | 43 | 0.017114914 | 0.058186739 | 3.399768026 | | | | 1148 | 50 | 4.355400697 |
| | ALC12 | 2 | 100 | 1 | 539 | 19 | 0.01 | 0.035250464 | 3.525046382 | | | | 639 | 20 | 3.129890454 |
| | ALC12 | 3 | 302 | 9 | 971 | 43 | 0.029801325 | 0.044284243 | 1.485982378 | | | | 1273 | 52 | 4.084838963 |
| | ALC17 | 4 | 664 | 88 | 912 | 270 | 0.13253012 | 0.296052632 | 2.233851675 | | | | 1576 | 358 | 22.71573604 |
| | ALC17 | 5 | 367 | 53 | 1034 | 244 | 0.144414169 | 0.235976789 | 1.634027955 | | | | 1401 | 297 | 21.19914347 |
| | ALC17 | 6 | 190 | 12 | 557 | 76 | 0.063157895 | 0.136445242 | 2.160383004 | 2.406509903 | 0.868582 | 0.004801348 | 747 | 88 | 11.78045515 |
| **STAT5A.2** | ALC12 | 1 | 570 | 23 | 808 | 71 | 0.040350877 | 0.087871287 | 2.177679724 | | | | 1378 | 94 | 6.821480406 |
| | ALC12 | 2 | 388 | 15 | 489 | 64 | 0.038659794 | 0.130879346 | 3.385412406 | | | | 877 | 79 | 9.007981756 |
| | ALC18 | 3 | 615 | 89 | 942 | 261 | 0.144715447 | 0.277070064 | 1.914585272 | | | | 1557 | 350 | 22.47912653 |
| | ALC18 | 4 | 617 | 98 | 561 | 223 | 0.158833063 | 0.397504456 | 2.502655608 | 2.495083253 | 0.640434 | 0.001027725 | 1178 | 321 | 27.24957555 |
| **STAT6** | ALC19 | 1 | 97 | 12 | 476 | 105 | 0.12371134 | 0.220588235 | 1.783088235 | | | | 573 | 117 | 20.41884817 |
| | ALC19 | 2 | 182 | 47 | 345 | 103 | 0.258241758 | 0.298550725 | 1.15609004 | | | | 527 | 150 | 28.4629981 |
| | ALC19 | 3 | 452 | 56 | 542 | 115 | 0.123893805 | 0.212177122 | 1.712572483 | | | | 994 | 171 | 17.20321932 |
| | ALC19 | 4 | 313 | 20 | 416 | 64 | 0.063897764 | 0.153846154 | 2.407692308 | 1.764860766 | 0.512152 | 0.020296067 | 729 | 84 | 11.52263374 |

**Table S2. Secondary antibodies**

| Species and fluorophore | Catalogue code |
|---|---|
| Donkey anti-mouse 488 | A21202 |
| Goat anti-chick 488 | A11039 |
| Donkey anti-goat 488 | A11055 |
| Donkey anti-rabbit 488 | A21206 |
| Donkey anti-mouse 546 | A10036 |
| Donkey anti-rabbit 546 | A10040 |
| Donkey anti-goat 555 | A21432 |
| Goat anti-hamster 568 | A21112 |
| Donkey anti-rat 594 | A21209 |
| Donkey anti-mouse 647 | A31571 |
| Donkey anti-rabbit 647 | A31573 |
| Goat anti hamster 647 | A21451 |
| Goat anti-rat 647 | A21247 |

## Supplementary Materials and Methods

### Measurement of protein expression levels

A custom macro (below) for ImageJ was used for quantification of protein expression. To install the plugin, put the file in the `Fiji.app/Plugins/' folder and restart Fiji or run `Help/Refresh' menus. To access the relevant part of the filesystem under MacOS, Ctrl-click on the Fiji application icon to open the contextual menu and click `Show Package Contents'.

Click here to Download macro file